Numerical Methods for the Primitive Equations (Space)

Fedor Mesinger and Zaviša I. Janjić*
UCAR Visitor Scientist Program, National Meteorological Center, Washington, DC 20233, U.S.A.

1. Introduction

A number of approaches can be taken in attempting to review methods for space discretization of the atmospheric primitive equations. A historical account of the achievements during the past 10 years of operational medium-range forecasting is one possibility and a general overview of the methods used another. But in view of the availability of other material such as the GARP Publications Series volumes on numerical methods (Mesinger and Arakawa 1976, WMO/ICSU 1979), the proceedings of the ECMWF 1983 seminar (ECMWF 1984) as well as those of the ECMWF workshop on horizontal discretization published only about a year ago (ECMWF 1988) perhaps the best we can do in a one hour lecture is attempt to review very recent work as well as concerns which currently exist regarding various aspects of space discretization. Our shopping list of developments and issues to talk about will in fact be rather like the Report of Working Group 1 of the mentioned workshop and is as follows.

- *The spectral transform method.* While most medium-range modelers are perhaps generally pleased with the performance and capabilities of the spectral transform method for global discretization concern is being expressed regarding the increase in relative computational cost of the Legendre transform as the horizontal resolution is increased. Accordingly, reexamination of the spectral technique against possible competing techniques is receiving a renewed attention (e.g., ECMWF 1988, Report of Working Group 1).

- *Semi-Lagrangian schemes.* A number of benefits has been demonstrated to come or is expected to come from the use of the semi-Lagrangian schemes. They offer the prospects of economy through time steps not limited by the CFL condition and do not suffer from the pole problem of the currently used finite-difference methods. Accuracy in the advection of spatially rapidly varying fields (e.g., moisture) is yet another feature that hopefully can be achieved (e.g., Williamson and Rasch 1988, 1989).

---

* Lecture presented by F. Mesinger (present affiliation: Institute of Meteorology, College of Physics, Belgrade, Yugoslavia)

- *Representation of sharp gradients.* Difficulties with the generation and advection of sharp features is a long-standing problem of the finite-difference method. More recently attention has been focused on the need to avoid creating new minima and also new maxima in the linear advection process. Characteristic-based techniques developed and extensively used outside meteorology seem to represent a very powerful method free of such problems.

- *Forcing at individual grid columns.* Methods used for horizontal discretization in weather prediction models have serious deficiencies in treating forcing performed at individual grid points (points of the transform grid of spectral method) and yet changes due to parameterization of physical processes are applied at individual grid points. In a recent paper (Janjić and Mesinger 1989) we have demonstrated that a given single grid point forcing can have a profoundly different effect for two types of horizontal discretrization both of which are commonly used in prediction models.

- *The pole problem.* The polar filtering used in latitude-longitude global finite-difference models is time consuming and obviously not appealing also for other reasons (e.g., filtering of some of the effects of physical forcing). In addition, the mere coverage of the sphere in a latitude-longitude fashion involves a computational overhead of more than 50 percent ($\pi/2$) compared to a hypothetical uniform grid.

- *The sigma system problem.* We have repeatedly written on the pressure gradient force errors in finite-difference sigma system models (e.g., Mesinger and Janjić 1987b). In a recent note (Janjić 1989) it was shown that in a number of examples use of the spectral method was associated with the pressure-gradient force errors in the rms sense larger than those of a simple finite-difference scheme. Other sigma system problems are known (Simmons and Burridge 1981; Simmons and Strüfing 1981) or being looked into (Bleck and Peng 1989).

- *Conservation of integral quantities.* Since its introduction by Arakawa (1966) the principle of the conservation of chosen integral quantities in particular of enstrophy and kinetic energy in order to control the energy cascade has perhaps been gaining a steadily increasing recognition. Possibilities for the maintenance of various properties of the continuous equations are associated with the choice of the horizontal grid however and it is only for (Arakawa) grids C and B/E that advection schemes enforcing a strict control of the energy cascade were shown possible (Arakawa and Lamb 1981; Janjić 1984). But there are examples of the nonstaggered grid being chosen for its reported ease of the

implementation of the fourth-order accuracy schemes (Purser and Leslie 1988).

In the remaining part of this lecture we shall
(a) discuss at somewhat greater length each of the listed issues, at the same time reviewing some recent as yet unpublished work (in particular work on the characteristic-based techniques and on the pressure gradient force errors of the spectral transform method), and
(b) show examples and some verification statistics of forecasts believed to derive their success relative to control forecasts primarily as a result of the differences in space discretizations used. The forecasts will be of

(1) an outbreak of a very cold air into mid-western United States in early February 1989, and

(2) convective precipitation patterns during the period 16 June - 5 July 1989, including the landfall and about four days of quasi-stationary movement over southern Texas and Louisiana of the tropical storm Allison.

2. *The spectral transform method*

In the present ECMWF T106 operational code Legendre transform takes about one fifth of the total computation time. If no new developments are forthcoming and the resolution of the next operational model is T213 or similar this fraction will increase to somewhat over two fifth of the time (Simmons, personal communication).

Two alternatives to the spectral transform method have recently been considered by Browning et al. (1989). One of them was a "vector-transform" method, formulated in terms of the horizontal velocity components rather than in terms of the vorticity and divergence. This avoids raising the differential order of the equations. The Legendre transform is not avoided but the authors nevertheless find that the operation count for the vector method is about 30 percent lower than that for the conventional spectral method.

If a uniform accuracy over all of the globe is not required one can take advantage of the conformal transformation of Schmidt so as to achieve a higher resolution over the area of interest only. This has recently been tested in a global shallow water model by Courtier and Geleyn (1988).

Various options being considered it may be appropriate to have a more general look at the properties of the spectral method irrespective of the matter of economy. Two of its most impressive features which have led to the current widespread adoption of the method for medium range forecasting are those of the method having

* no phase speed error in linear advection; and
* no pole problem.

On the other hand, we believe that as it is customarily used the method is not free of aspects to be concerned about, as follows.

* Effects of "physics" are calculated on the transform grid which is not completely resolved in spectral space. It is thus to be expected that in each transformation some of the effects of physics are lost. One alternative to over-resolution (to avoid aliasing) is in fact being used, although not in weather prediction models; it is exact energy conservation (e.g., Farge and Sadourny 1989).

* The method is known to have some numerical problems: the Gibbs phenomenon, and as mentioned and will be elaborated in more detail later, errors of the pressure gradient force.

* The method has little regard for the physical content of the governing equations. It is based on the idea of global representation using chosen basis functions. This is in conflict with the parameterization of physical processes in which values at points of the transform grid are treated as volume averages. Note that a simple two-point finite-difference quotient is less subject to this objection since for two neighboring points its value is consistent with the interpretation of grid point values as volume averages.

3. *Semi-Lagrangian schemes*

In recent years a very substantial effort has been devoted to the development of semi-Lagrangian schemes. They can be (and have been, or are being) applied in finite-difference, spectral and finite-element models. As stated, three objectives have and are being pursued: economy, removal of the pole problem of finite-difference methods, and accuracy in the advection of spatially rapidly varying quantities (e.g., moisture, cloud water, turbulent kinetic energy and, perhaps, some contaminants that one might wish to monitor in the model).

The essence of the semi-Lagrangian schemes is discretization along trajectories and they are thus a combination of space and time differencing. They will for this reason also be covered in the lecture by Burridge further in this volume. We shall therefore restrict ourselves to comments which we feel are needed for putting the remaining parts of our lecture in perspective.

Starting with the pioneering work of Robert (1981, 1982) and Bates and McDonald (1982) it has been repeatedly demonstrated using various designs of the semi-Lagrangian schemes that successful integrations are possible with very long time steps. Tests have been performed either in idealized cases with

a small scale disturbance being advected by the large scale flow, or, alternatively, in complex atmospheric models. For time steps which were not excessively long no visible loss in accuracy has been reported.

If however in reality there are appreciable velocity changes with time scales less than the chosen time step accuracy of the trajectory calculation will be poor. The accuracy of the trajectory calculations being thus the critical point with long time steps, the tests with small scale disturbances advected by large scale flow do not improve our understanding of the possible problems with such schemes. On the other hand, the effects of the application of semi-Lagrangian schemes in complex models are obscured by the presence of a number of other processes so that important errors occurring at some places some of the time may be hard to notice. Regarding idealized tests, we believe that severe low resolution experiments like those of Sadourny (1975), Janjić (1984) or Rančić and Ničković (1988) would reveal if indeed there are no demerits of semi-Lagrangian schemes compared to sophisticated schemes based on other approaches.

Regarding models with comprehensive physics, we are concerned about the deceleration of gravity-inertia waves due to the use of very long time steps. This in turn leads to overestimation of the part of the forcing which remains in the large scale flow, and underestimation of the part which disperses away as gravity-inertia waves (Janjić and Wiin-Nielsen 1977). While our simulation of the geostrophic adjustment process may not today be entirely satisfactory one would like to expect that with still higher horizontal resolution and perhaps also better numerical schemes it shall eventually improve so that these issues may gain in importance.

One should moreover have in mind that the part addressed by the semi-Lagrangian approach is typically not the one most demanding in computer time. In comprehensive prediction models physics tends to be more expensive than the dynamics, and physics can hardly be expected to become simpler as the models are refined. Physics however can be and frequently is performed at a variety of time steps chosen for physical and not for computational reasons. In say the National Meteorological Center (NMC) eta model, to be outlined in more detail later, with physical parameterizations typical of the state-of-the-art models physics takes more than two thirds of the total computation time in spite of being highly optimized in terms of coding and various time steps used. Gravity-inertia and advection parts which are limited by their respective CFL conditions take about one fourth of the time. Thus, possibilities for savings in eliminating the CFL restrictions on these parts of the code are modest.

It is only somewhat later in the development of the semi-Lagrangian schemes that their ability of removing the pole problem of global finite-difference models has been emphasized (McDonald and Bates 1988; Bates et al. 1989). As stated, the latitude-longitude grid along with a filtering procedure is associated not only with a severe computational expense but also with a degradation of the numerical solution. The most recent discussions of the subject may be those of Purser (1988a, 1988b).

Improved accuracy in the advection of spatially rapidly varying fields is yet another objective of the work on the semi-Lagrangian schemes (e.g., Williamson and Rasch 1989; Rančić and Sinđić 1989). As this objective is common to a variety of methods we shall cover it as a separate subject, in the following section. In doing this we shall however not emphasize the semi-Lagrangian approach since to the extent this is possible at the present stage it has been amply covered at a variety of other places. Note, for example, the already mentioned proceedings of the ECMWF workshop on techniques for horizontal discretization (ECMWF 1988).

4. *Representation of sharp gradients*

Increasing the spatial resolution is of course the most straightforward way of trying to improve the representation of rapidly varying fields. To make the idea practical one can limit the area over which the resolution is increased; the extreme solution of this type obviously are limited area models. A possibility of achieving a continuously varying resolution in global spectral models has already been mentioned (Schmidt 1977; Courtier and Geleyn 1988). Similar solutions have already earlier been tested in a finite-element model (Staniforth and Mitchell 1978), and in a global finite-difference model (Sharma et al. 1987).

A related approach which appears to be receiving a vigorous attention recently is one of choosing the area over which the resolution is increased not on geographical grounds but on the basis of flow properties. These are the so-called "adaptive methods". According to Skamarock (personal communication) one can distinguish between three kinds of adaptive schemes, as follows.

* Passive schemes. "Passive" would refer to a scheme whereby the mesh refinement is occurring as a result of flow evolution, rather than as a result of a decision-making algorithm. An example of a passive scheme is the isentropic coordinate model: coordinate surfaces approach each other in regions where an increased resolution is presumably needed, such as frontal zones. Isentropic coordinate models are of course appealing also from the point of view of the conservation of potential vorticity, and keep enjoying a considerable degree of attention for more than two decades. The most recent references may be those

of Hsu (1988) and Bleck and Peng (1989).

* "Local" refinement method. With this method estimates of truncation error are made, and subsequently higher resolution subgrids are added or deleted depending on the space distribution of high truncation error points (e.g., Skamarock et al. 1989; Skamarock 1989; Skamarock and Klemp 1989).

* "Global" refinement method. With the global method existing grid points are redistributed from regions of small to regions of large solution variations (Dietachmayer and Droegemeier, personal communication).

As truncation error in comprehensive atmospheric models is completely dominated by physical parameterizations, it would seem that tests with fully-developed models are going to be critical regarding possible benefits from the last two types of adaptive methods.

A requirement more specific than that of an increased truncation error type accuracy is for the advection scheme not to create negative values during advection of physically positive quantities. A simple upstream scheme of course satisfies that requirement but is not a scheme to use if preservation of sharp features is also desired. Efforts at designing schemes which would be "positive definite" but at the same time perform better in treating sharp features were many, in meteorology starting perhaps with the work of Smolarkiewicz (1983, 1984). For subsequent references see e.g., Bott (1989).

More recently it was realized that preventing false amplification of maxima may be just as important since the overshoot can erroneously interact with the parameterizations and produce, for example, spurious precipitation (Williamson and Rasch 1988). Consider, for illustration, the specific humidity (q) vertical advection scheme

$$-\dot{\eta}\frac{\partial q}{\partial \eta} \rightarrow -\frac{1}{2\Delta\eta}\left[\dot{\eta}_{k+1/2}(q_{k+1}-q_k) + \dot{\eta}_{k-1/2}(q_k-q_{k-1})\right] \qquad (4.1)$$

where η is the vertical coordinate (σ modified to have quasi-horizontal coordinate surfaces, Mesinger 1984), full values of indices refer to model layers and half-values to interfaces. This, in fact, was the scheme used in the mentioned eta model (Janjić and Black 1987; Mesinger et al. 1988), with the addition of a check for negative moisture so that the "fluxes" in the brackets of (4.1) would be altered to the extent needed to keep the moisture positive and at the same time the vertical sum of fluxes constant. Suppose however that locally in the direction of $-\eta$ a downward step in the distribution of moisture exists as sketched in Fig. 4.1 and the η vertical velocity in the region shown is constant and negative. Inspection of (4.1) shows that at the layer k this would

lead to an appearance of a false maximum in the distribution of q. This might result in condensation and an enhancement of upward velocity, thereby setting up an instability-like positive feedback mechanism.

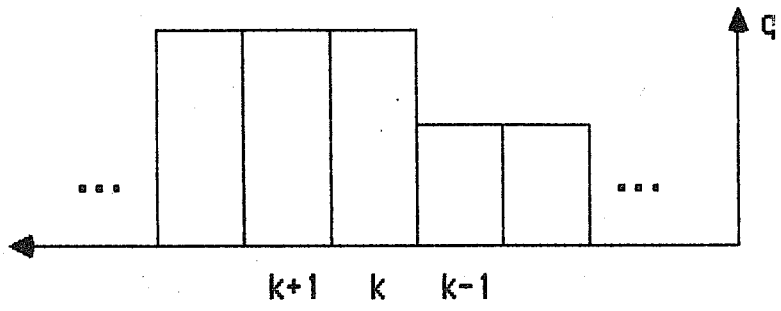

Fig. 4.1. Schematic illustration of the vertical distribution of the specific humidity for which a spurious increase in the maximum value is possible due to the vertical advection scheme.

This indeed must have been happening in the eta model when it was run for situations of spring 1988. Monitoring the performance of the model at that time a repeated occurrence of areas of concentrated and excessively intense precipitation ("bulls eyes") was noticed, as shown in Fig. 4.2. Each of the three centers seen in the figure was associated with a sea level pressure minimum of the depth clearly not supported by observations. Suspecting that the problem was the described spurious precipitation increase (4.1) was replaced by a scheme based on rewriting its left side as

$$-\frac{\partial(\dot{\eta}q)}{\partial\eta} + q\frac{\partial\dot{\eta}}{\partial\eta}. \qquad (4.2)$$

For the first term of (4.2) the "first-order upstream-centered" scheme of van Leer (1977) was used. It consists of the advection of the histogram of q by the interface η velocities followed by a determination of new layer averages. For constant eta vertical velocities this scheme reduces to the upward scheme. A simple centered second-order scheme was used for the second term of (4.2). If the eta vertical velocity is constant (linear advection) and if the CFL condition is observed the described scheme guarantees that neither new maxima nor new minima of q will be created in the advection process.

Tests have indeed demonstrated that precipitation of some of the bulls eyes was reduced substantially due to the use of this scheme, as shown in Fig. 4.3. The two centers over water now show much more credible amounts, with the maximum value at the center off the coast of Cuba reduced by more than half of

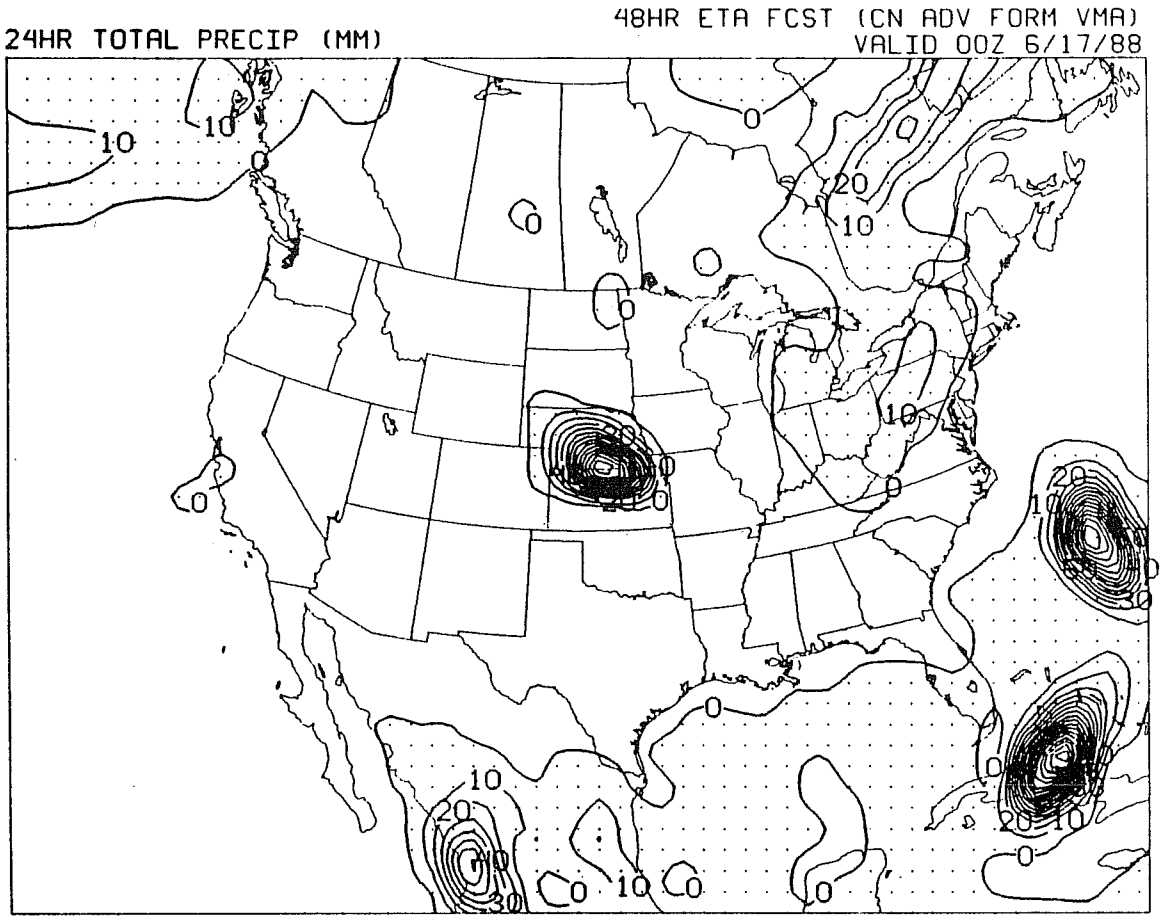

Fig. 4.2. 48 h forecast of 24 h accumulated precipitation, verifying at 0000 UTC 17 June 1988. The values shown are millimeters in 24 h.

its amount of over 170 mm/24 h seen in Fig. 4.2. The center on the border between Kansas and Nebraska is however still too intense, showing the maximum value of over 110 compared to over 130 mm/24 h in Fig. 4.2. This residual tendency for too intense precipitation maxima was subsequently removed by the refinement of the Betts-Miller cumulus convection scheme.

With the changes in the moisture advection and in the cumulus parameterization scheme done in reverse order sensitivity to the moisture advection scheme was reduced but not eliminated. Several tests of this type were made; typically, higher precipitation amounts obtained at intensive centers using (4.1) were then associated with sea level pressure values lower by about 1-2 mb. In one case the difference amounted to more than 2 mb. In all of the cases considered which were verifiable against the routinely prepared NMC surface analyses the

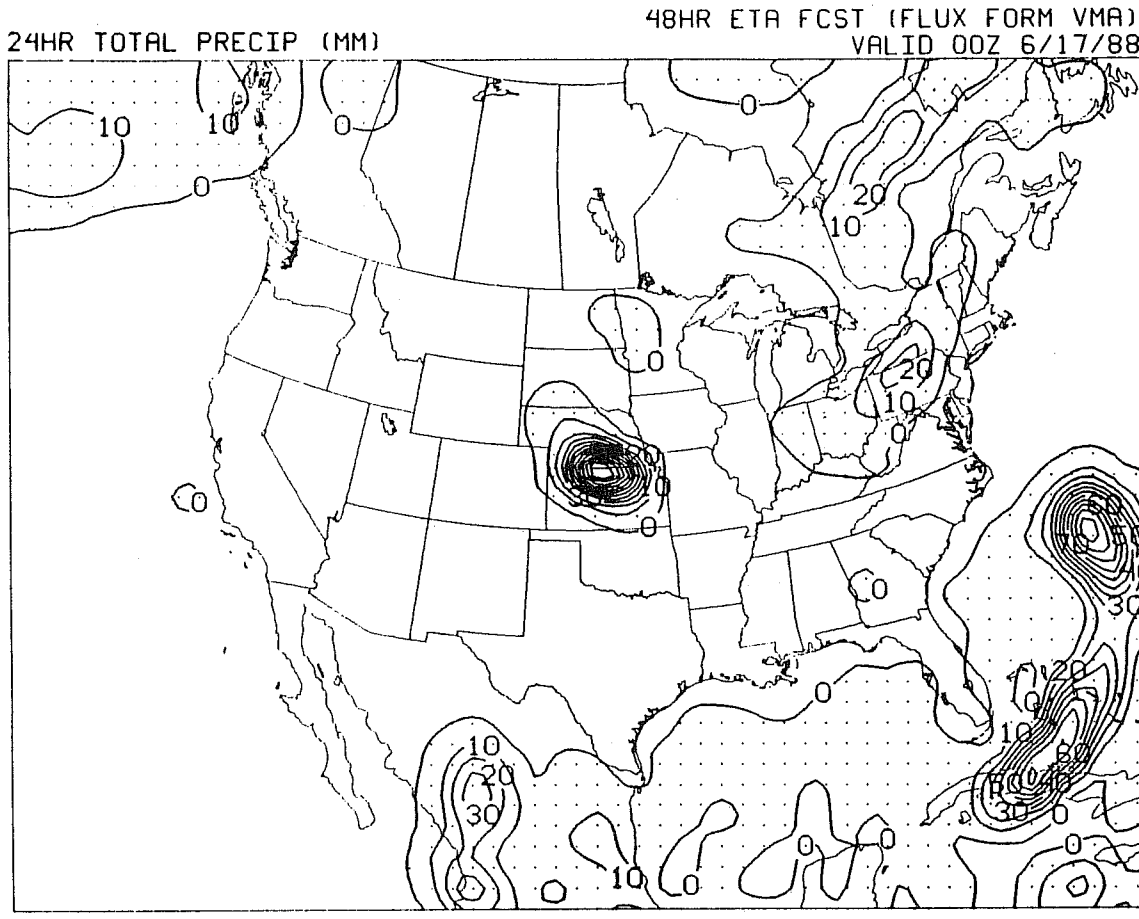

Fig. 4.3. As in Fig. 4.2 except that the scheme for the vertical advection of moisture described in the text was used.

shallower low centers of the forecasts made using the scheme based on (4.2) agreed better with the analyses.

Note that the described "histogram advection" scheme is based on the assumption of constant values of the advected quantity within the layers. It is in this respect a version of the so-called "piecewise constant" method introduced by Godunov (1959). Later tests with the eta model have indicated benefits from a higher accuracy method in which prior to translation humidity histogram is modified so as to locally minimize steps by permitting a linear change of q across layers. Thus, this is a "piecewise linear" method. To guarantee that neither new maxima nor new minima be generated in the translation step the change of q across layers is subject to the restriction that it not generate new maxima and new minima in the humidity profile. This is the so-called monotonicity constraint (van Leer 1977).

The scheme is applied in the eta model in the following manner. As the first step of the slope adjustment procedure maxima and minima in the profile of q are identified. Slopes in these layers are not changed. For efficient vectorization slopes in the remaining layers are adjusted in an iterative procedure. With average values within layers kept constant in each sweep end points of the linear segments of the q profile across these layers which are at the side of the smaller of the two steps at its interfaces are moved to the mid-points of that step. This is illustrated in Fig. 4.4. The dotted line in the figure represents a hypothetical profile of q prior to the adjustment procedure. As the first step of this procedure values at layers k and k+3 would be identified as a minimum and as a maximum, respectively, and flagged not to be changed. Slopes which layers k+1 and k+2 would obtain as a result of the first sweep of the slope adjustment are shown by the two full lines in the figure. The code is at present set to have three iterations performed since inspection has shown that after three iterations little in view of adjustable steps remains and that computer time demands of three iterations are modest.

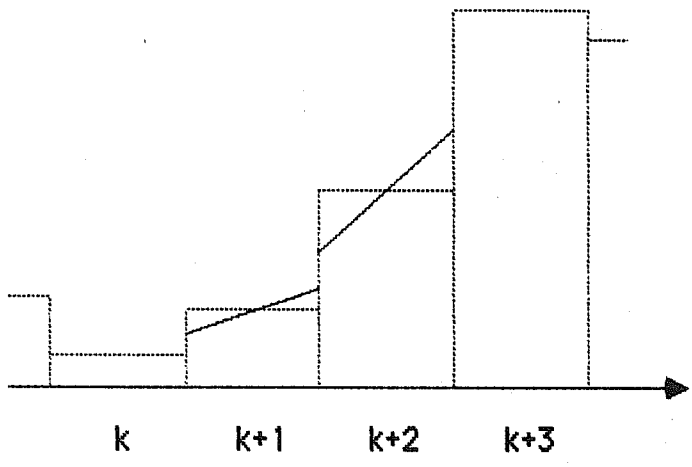

Fig. 4.4. Schematic illustration of the slope adjustment procedure of the eta model moisture advection scheme. The dotted line shows the original histogram of q. The full lines show the distribution of q in layers k+1 and k+2 following the first sweep of the adjustment code.

The described schemes are in fact Eulerian advection problem versions of a much more general class of schemes referred to as Godunov-type schemes, or characteristic based schemes. They have been developed with the objective of simulating flows which contain discontinuities, such as shock waves. Most of this work has been done in the fields of aerodynamics and astrophysics; applications to problems in meteorology are so far few and very recent

(Priestley 1988; Carpenter et al. 1989). The method was introduced by Godunov (1959) by taking advantage of the solution to the so-called Riemann's problem. This problem describes evolution of the fluid initially containing two constant states in a tube, separated by a discontinuity. As introduced by Godunov, these two features at the same refer to the two basic aspects of the method: the fluid is represented by piecewise constant functions, and interactions at the boundaries of zones of constant states are calculated using the solution to the Riemann's problem. This involves propagation of appropriate quantities along the characteristics of the system.

Van Leer has refined Godunov's method by introducing the piecewise linear method for the advection problem (1977) and for fluid dynamics (1959). With his approach the slope of a variable within each zone (grid box) is defined based on the values at neighboring zones, say as with the procedure illustrated in Fig. 4.4. A still more accurate "piecewise parabolic" (PPM) method was introduced by Colella and Woodward (1984). It was applied recently to one- and two-dimensional advection as well as to a convection problem by Carpenter et al. (1989) and compared with a number of finite-difference methods.

Note that the outlined Godunov-type methods are <u>not</u> finite-difference methods. With these methods space derivatives are never approximated by finite-difference quotients or by similar approximations based on series expansions. Derivatives within the advection terms are handled through the Lagrangian treatment of the advection process so that advection of the boundaries of fluid elements occupying grid boxes at the beginning of the time step is calculated and once the time step is completed variables are interpolated back to the original grid ("Eulerian remap", Carpenter et al. 1989).

Having no assumptions about space derivatives Godunov or characteristic based methods avoid an inconsistency which exists between dynamics and physical parameterizations in present weather prediction models. Namely, in space discretizations grid point values or their equivalent in spectral methods are treated as point samples of continuous functions. Parameterization schemes, on the other hand, treat grid point values as grid box averages. Disretization methods are thus in conflict with the parameterization schemes and as a result some of the effect of parameterizations is invisible to the dynamics. As hinted already, we suspect that the conflict may be particularly harmful in currently used spectral methods because of their additional problem of over-resolution in physical space. For finite-difference schemes, we have demonstrated recently (Janjić and Mesinger 1989) that in an idealized example the error can be substantial. Being free of such errors, characteristic based methods look to us

as a very attractive candidate for eventual application to the weather prediction problem.

Carpenter et al. in their paper present three cases of 1-D advection and one of 2-D advection. In these they compare results obtained using PPM (with and without a "steepening" procedure) with piecewise constant and piecewise linear advection, and with two finite-difference schemes, fourth-order leapfrog and a version of Smolarkiewicz' (1984) positive definite scheme. 1-D tests were of the advection of a rectangular wave, of a triangular wave, and of a Gaussian distribution. The relative strength of the piecewise linear method and of PPM compared to other methods was particularly evident in case of the rectangular wave, as shown in Fig. 4.5. Problems of the reduction or of an increase in the maximum value of the wave, or of the noise, are absent in the plots of the three lower panels. They differ only in their ability to maintain the steepness of the wave. With these three schemes, the greater the computational effort better is seen to be the preservation of the steepness of the wave.

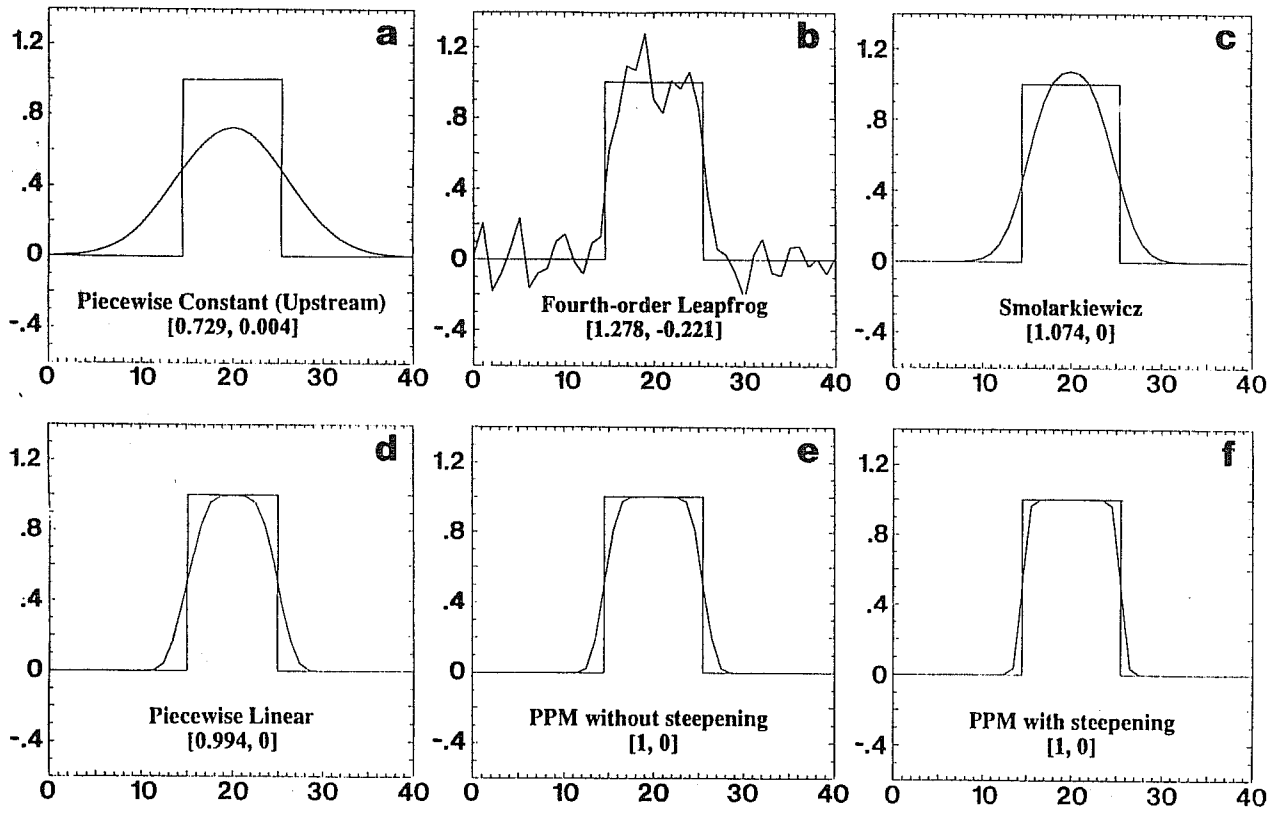

Fig. 4.5. Solution of the 1-D linear advection equation in which a rectangular wave of unit height is advected toward the right in a domain of 40 grid points and periodic boundary condition (Carpenter et al. 1989). The true solution is shown after 1.25 revolutions (100 time steps) along with solutions using various schemes as indicated on the plots. Quantities in brackets are maximum and minimum values, respectively.

Results of Carpenter et al. for the 2-D advection tests are shown in Fig. 4.6. The initial condition, due to Zalesak (1979), is now shown as a separate plot in the upper left panel of the figure. Results for the fourth-order leapfrog scheme are missing because of the difficulties the authors had with the stability of the scheme. Piecewise linear solution is this time of a similar quality to that using Smolarkiewicz' scheme: the groove is more eroded but the sides of the cylinder are steeper. Resemblance of the PPM solutions in particular of that with the steepening procedure to the initial condition is remarkable.

As a test of fluid dynamics application Carpenter et al. have made a number of 2-D simulations of a buoyant thermal. Rising of the thermal in an inviscid and isentropic fluid was considered. In a half-domain of 1.6 by 4 km the initial bubble had a radius of 1 km and a potential temperature excess of 2 K at its center which decreased smoothly to 0 K at its edge. Rigid, free-slip and non-conducting boundary condition was used. Grid distance of the control experiment was 20 m; the computational grid thus consisted of 200 × 80 zones. This was hoped to be adequate for an explicit representation of turbulent processes and no parameterization of turbulence was present.

The evolution of the thermal in the control experiment of Carpenter et al. (denoted PPM-20S, 20 referring to the grid size and S to "small" integration region) in its later complex stages is shown in the upper panels of Fig. 4.7. Departure of the potential temperature is shown, at contour intervals of 2 minutes. The same fields obtained in a simulation using a finite-difference model are shown in the lower panels of the figure. This is a staggered grid second-order accuracy model developed by Droegemeier and Wilhelmson (1987) with some diffusion aimed at controlling the nonlinear instability.

Impressive sharpness as well as a variety of features is seen in the PPM plots neither of which is to the same degree present in the finite-difference (DW) result. In particular, migration of the potential temperature maximum away from the symmetry axis is missing in the DW result. Carpenter et al. argue that this migration is caused by the rigid boundary and note that it has been observed in other numerical studies. Because of this difference the PPM result shows two entraining vortices in the upper part of the plume at 14 and 16 minutes, compared to only one at 16 minutes in the DW result. In the PPM result the descending branch of the thermal is distorted by a series of Kelvin-Helmholtz instability features which are absent in the DW result.

The reader is referred to the paper by Carpenter et al. for results on PPM experiments with degraded resolution, with piecewise linear and with

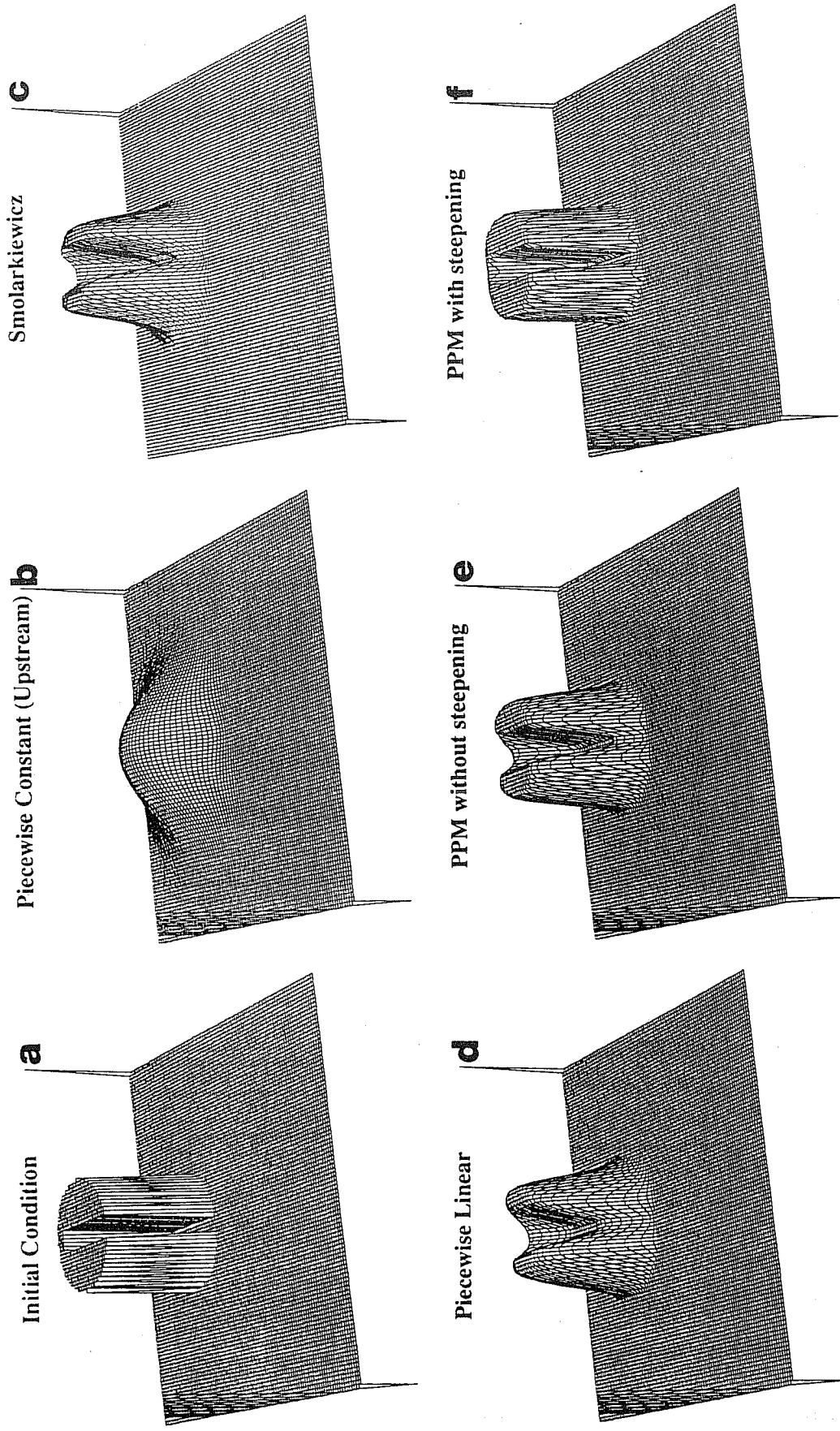

Fig. 4.6. Solution of the 2-D linear advection equation in which a grooved cylinder of unit height undergoes solid-body rotation one revolution in a 100 x100 grid. (a) Initial condition, (b)-(f) various schemes as noted in the figure. The spikes in the foreground and background are -0.5 and 1 unit high, respectively. From Carpenter et al. (1989).

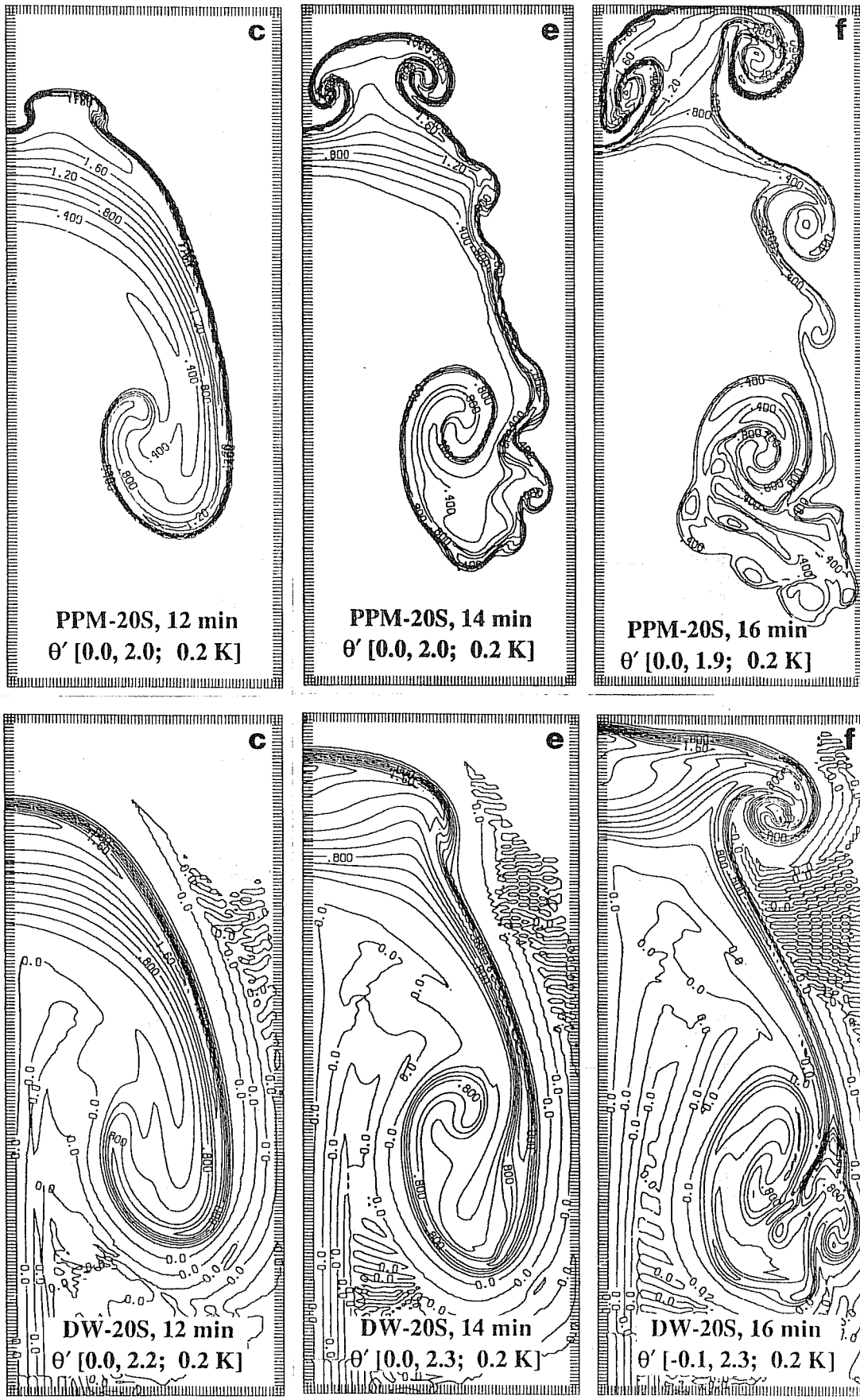

Fig. 4.7. Departure of potential temperature (deg K) for the control experiment of Carpenter et al. (1989) at 12 min, 14 min and 16 min after the initial time (upper panels). As above, but using the finite-difference model of Droegemeier and Wilhelmson (lower panels). Figures in square brackets show minimum value, maximum value and the contour interval, respectively.

piecewise constant interpolation, and with a larger domain. They also provide extensive diagnostics. Comparing the PPM results with degraded resolution against DW results Carpenter et al. conclude that PPM yields a qualitatively comparable solution at half the spatial resolution of the DW model. At the same time, at this difference in resolution the two codes were taking similar amounts of computer time. However, the DW code they used was taking advantage of two efficiency stratagems, time splitting and artificial sound speed reduction, which were not available to their PPM code. With these two techniques eventually introduced into the PPM according to Carpenter et al. the two could become about equally demanding of computer time at the same resolution. In this case the benefit resulting from PPM would come with no or with little demands for an increase in computing power.

It is our impression that PPM looks as a very attractive candidate for experimental work with full primitive equations with a view towards eventual application in weather prediction. It may not be obvious what improvements one might hope for. Elimination of the problem to be pointed out in the following section is one possibility.

5. *Forcing at individual grid columns*

As noted, an inconsistency exists between the methods used for physical parameterizations and those used for space discretization in weather prediction models. In physical parameterizations, grid point values are treated as mesh (grid box) averages. In space discretization, they are treated as point samples of continuous functions.

For an estimate of a possible magnitude of the problem we have performed numerical experiments using two grids commonly used in weather prediction models. Results have already been reported in an ECMWF publication as well as published (Janjić et al. 1988; Janjić and Mesinger 1989) so we shall summarize them only very briefly here. Shallow water integrations were performed using two limited area models with the Coriolis terms included. One of the models was defined on the staggered C grid, and the other on the semi-staggered E/B grid. For each grid, experiments were performed with grid sizes of 250, 125 and 62.5 km. A source and a sink, of constant intensity, were placed symmetrically at two sides of the central part of the domain. They covered, for the three resolutions considered, areas on one, four and sixteen grid points, respectively.

Deviation from the mean height at the sink after 24 hours is shown in Fig. 5.1. For the 125 and 62.5 km resolutions the values shown are averages over the

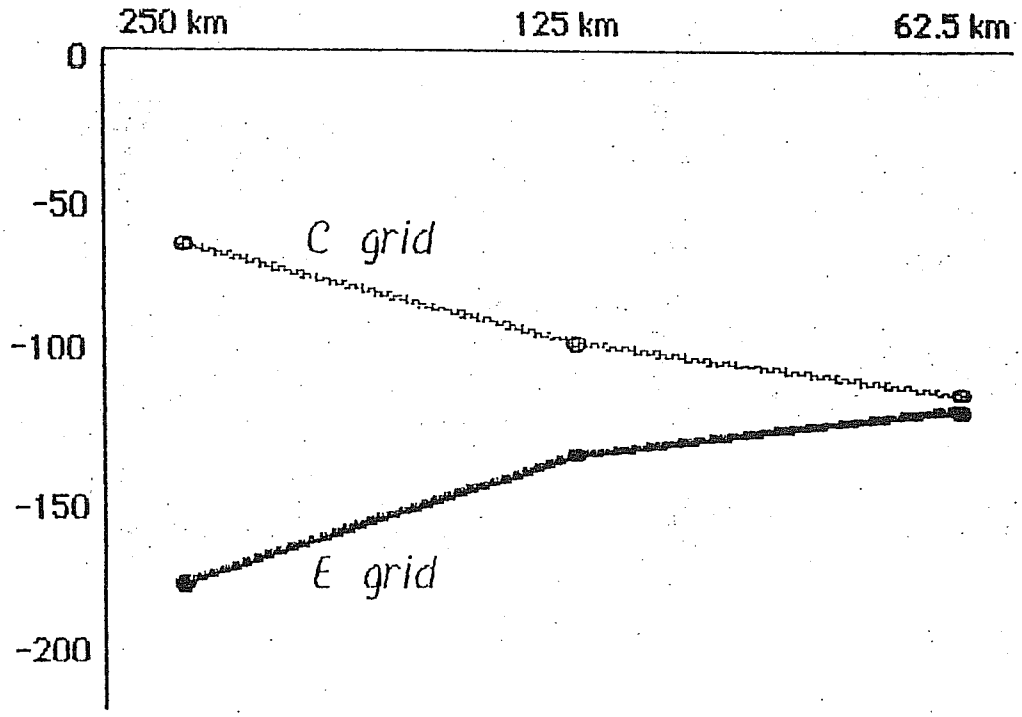

Fig. 5.1. Deviation from the mean height at the sink point after 24 h of forcing in the case of 250 km experiments, and the deviations from the mean height averaged over four and sixteen points of the sink in the cases of 125 and 62.5 km resolutions, for the C grid (light solid line) and the E grid (heavy solid line).

four and over the sixteen points of the sink. At the lowest resolution substantial differences are seen in the depth of the sink on the two grids. The differences are very much reduced in the two 125 km experiments and are virtually absent in the highest resolution, 62.5 km experiments.

Assuming the asymptotic value to approximate the true solution, each of the models is seen to be grossly in error with forcing at a single point. Yet it is very much through forcing at individual grid points that most of the physical parameterizations are performed in weather prediction models.

Perhaps the large error obtained in our experiment is not representative of the situation which generally exists in models. But even if the typical error were to be much smaller and large errors occurred only occasionally it should still be helpful to reduce or eliminate them.

We can see three possibilities of trying to achieve this, as follows.

* With forcing kept at individual grid points, one could attempt to develop

parameterization schemes which would be consistent or approximately consistent with the appropriate part of space discretization. For example, in the source/sink experiment performed, for a constant intensity of the source and the sink the forcing actually applied at the source and the sink grid points would be designed around the grid and space discretization used so as to give an approximatelly correct result. This approach however would appear to require a reexamination of the energy and perhaps other conservation aspects of the space discretization.

* Parameterization schemes could be designed which would minimize or avoid forcing at single grid points. Instead, simultaneous forcing at several neighboring points would be performed. This idea was suggested a long time ago by Egger (1971) and has recently been applied in construction of the four-point mountains on the E grid (Mesinger 1985; Mesinger et al. 1988).

* PPM or PPM-like discretization for weather prediction models could be developed presumably able to handle the small scale forcing in a physically consistent way.

6. *The pole problem*

There are two aspects to the pole problem of the finite-difference models using the standard latitude-longitude grid, as follows.

* CFL condition requires a filtering procedure to avoid the need for excessively small time steps. Filtering is not only time consuming but in addition removes some of the effects of physical parameterizations performed on a dense grid in high latitude regions. Finally, the possibilities of detrimental effects on the accuracy of the schemes and of other spurious effects have to be considered (Purser 1988a; Takacs and Balgovind 1983).

* Irrespective of numerical problems, there is an overhead of having $\pi/2$ the number of points one would have in a hypothetical uniform grid on the sphere. The extra resolution in one direction and in some of the regions only is not likely to be of any help but is in fact the reason for the problems listed above.

A rather substantial effort has gone into grids which have the number of points along latitude circles decrease as the poles are approached, most notably into the well known "Kurihara" grid. The idea has recently been looked into again from the Taylor series type accuracy point of view (Purser 1988b).

We however are of the opinion that grids with geometrical regularity as needed to enable the design of schemes imposing various properties of physical relevance such as enstrophy conservation are a better candidate for achieving a high level of performance. At the same time we find it difficult to believe that

with all the demerits listed above the latitude-longitude grid is the final word on regular grids for the domain as simple as the sphere. It is true that a substantial effort has gone also into the design of schemes on quasi-homogeneous regular grids for the global domain such as the icosahedral-hexagonal grid (as reviewed e.g., by Williamson 1979). But these efforts were made in very early days of the development of numerical techniques for the primitive equations when little was known about various mechanisms of the spurious noise generation. Perhaps the hexagonal grid is indeed a questionable choice because of its problem of having three velocity component points for each mass grid point rather than two. But the expanded cube approach taken a long time ago by Sadourny (1972) we feel deserves a reexamination. The experiments of Sadourny were plagued by a noise problem. Considering therefore the possibility of an enstrophy conserving scheme he ends his paper stating that "this would require the use of a staggered grid, which may lead to larger truncation errors on the boundaries." But we now know that it is precisely the staggered grids, C or E/B, which are needed to use schemes that impose controls on false energy cascade and which have favorable geostrophic adjustment properties, features removing and reducing, respectively, the two major sources of spurious noise in primitive equation models.

There is a number of attractive features of the expanded cube grid additional to its quasi-uniform distribution of points. The cube can of course be expanded in such a way as to have all coordinate lines segments of great circles so that the curvature terms are eliminated. If its two vertices are placed to coincide with the two poles as done by Sadourny (Fig. 6.1) then all six of its sides are in the same position relative to the earth's axis of rotation. From the numerical point of view eight singular points and singular lines could be a source of difficulties. Note however that if say an E grid were to be used on each of the sides then the

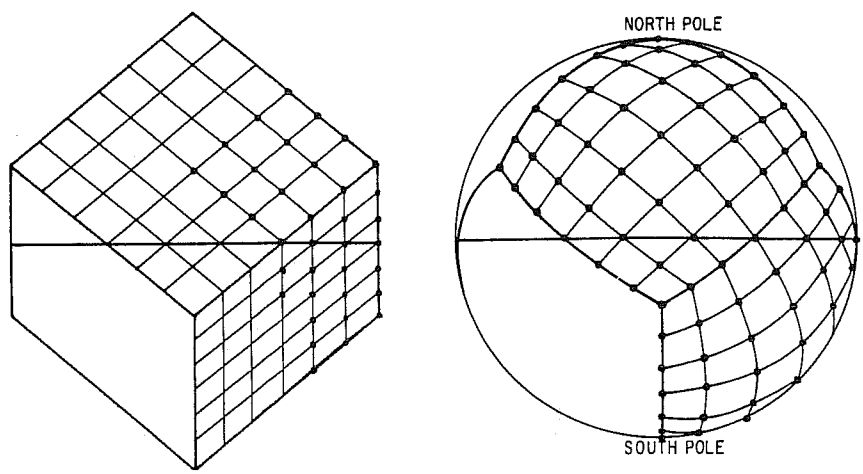

Fig. 6.1. A global grid obtained by expanding a cube to become a sphere; after Sadourny (1972).

eight vertex points would be surrounded by three velocity points each; three points would appear to be just the number needed for second order schemes to be noise free since a linear velocity change can fit three points exactly and not four. Conversion of a limited area code into an expanded cube model seems to be a relatively straightforward project in the sense that it can be broken up into a number of independent tasks. Use of a nonorthogonal coordinate system may be one more reason of concern; but some experience is as pointed out available (Sadourny 1972; see also references in Sharman et al. 1988) with no alarming results.

7. *The sigma system problem*

Reference has already been made to a number of problems associated with the use of the sigma system. Most attention has received the problem of the non-cancellation of errors of the two terms of the pressure gradient force in finite-difference models (e.g., Mesinger and Janjić 1987b). The pressure gradient force errors in σ-coordinate spectral models are perhaps often believed to be small or unimportant although little evidence has been published to support such a view.

The principal difficulty in assessing the significance of this and other σ-coordinate problems (advection, horizontal diffusion) arises due to the fact that a competitive technique for representing mountains in spectral models is missing.

Following Janjić (1989a), simple examples will be summarized here aimed at assessing the order of magnitude of the pressure gradient force errors in σ-coordinate spectral models, and at examining the spatial distribution of the errors. As usual, in these examples small-scale mountains were considered. For reference, the errors of a finite-difference scheme were also calculated. Calculations were performed for an idealized atmosphere following an example of Mesinger (e.g., Mesinger and Janjić 1987b).

The examples refer to a horizontally homogenous atmosphere at rest, and in hydrostatic equilibrium. In such an atmosphere the pressure gradient force is zero everywhere, and the computed pressure gradient force in a discretized system represents the error of the discretization method. Let the following information about this atmosphere be available in a vertical cross section along a constant latitude:

(i) Surface pressure p_S on an equidistant horizontal grid with M independent points;
(ii) Surface geopotential Φ_S on the same M-point horizontal grid; and,

(iii) Geopotential Φ on the same M-point horizontal grid, and on L_m equidistant σ levels.

Let us now consider the spectral horizontal representation in terms of trigonometric functions which is equivalent to the grid-point representation on the M-point grid. The term "equivalent" is used here to denote the requirement that the spectral representation have the same number of degrees of freedom as the grid-point representation, and yield the same values at the grid points of the M-point grid. This requirement will be satisfied if the coefficients of the truncated trigonometric series are computed using the approximate Fourier transform formulae.

In order to calculate the pressure gradient force error, spectrally represented temperatures on the σ levels are needed. Following e.g., Mesinger and Janjić (1987b), the temperatures are retrieved from the geopotentials. For this purpose we choose the hydrostatic equation introduced by Bourke (1974), which can be reformulated in the finite-difference form as

$$\Phi_L = \Phi_{L+1} + R[(T_{L+1}+T_L)/2]\ln(\sigma_{L+1}/\sigma_L), \quad \text{for } L < L_m;$$
$$\Phi_{Lm} = \Phi_S + R\{T_{Lm} + [(T_{Lm}-T_{Lm-1})/\ln(\sigma_{Lm}/\sigma_{Lm-1})]\ln(1/\sigma_{Lm})/2\}\ln(1/\sigma_{Lm}). \tag{7.1}$$

Here, Lm is the lowest model level. The other symbols used have their usual meaning.

The pressure gradient force error of the finite-difference method is calculated by the formula:

$$-\delta_x\Phi_\sigma - R\,\overline{T}^x\delta_x \ln p_S.$$

Here, the symbol δ_x, and the overbar with subscript x, denote the simplest two-point differencing and averaging operators applied in the zonal direction. The subscript σ indicates that the differencing is performed on a σ surface.

The geopotentials on the σ levels are calculated analytically from chosen continuous temperature profiles T(p). Following Mesinger (1982), two vertical temperature profiles are considered. The temperature at 800 mb level is taken to be 0°C in both cases, and it varies linearly with lnp, reaching, respectively, 10°C ("No inversion case") and -10°C ("Inversion case") at the 1000 mb level. Above 800 mb the two profiles coincide, decreasing linearly with the same lapse rate as in the no inversion case below 800 mb. This situation is

schematically shown in Fig. 7.1. Note that with the profiles chosen, the temperatures become unrealistically low at higher model levels. This, however, has no impact on the errors at the lower levels.

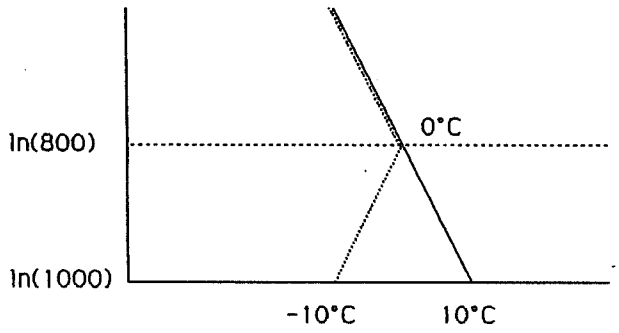

Fig. 7.1. Temperature profiles prescribed in the "Inversion" (dotted) and "No inversion" (solid) cases.

The numerical values of M and L_m used in the calculations are 120 and 15, respectively. In the main experiment, a single-grid-point mountain is located in the middle of the horizontal domain, i.e., at the point with the horizontal index M/2+1. The remaining part of the domain is assumed to be flat. The surface pressure is set to 800 mb at the top of the mountain, and to 1000 mb over the flat terrain. This experiment setup is identical to that of Mesinger (e.g., Mesinger and Janjić 1987b).

In order to examine the possible impact of the horizontal scale and the shape of the mountain, the experiments are repeated with three different shapes of the three-point mountain: a triangular mountain with the slopes linear in lnp, an obelisk-shaped mountain, and a trapezoidal mountain (three-point elevated plateau). Note that the single-point mountain and the trapezoidal three-point mountain can be considered as extreme cases of the obelisk-shaped mountain. The triangular mountain can also be viewed as a special case of the obelisk-shaped mountain. The surface pressures at the tops of the three-point mountains are again set to 800 mb. In the case of the obelisk-shaped mountain, the surface pressures at the two mountain points other than the top point are [1000 - 200 exp (-.25)] mb = 844.24 mb.

The single-point mountain and the three-point mountains are shown schematically in Fig. 7.2. As indicated in the figure, with the currently used horizontal resolution, the widths at the bases of the single-point, and the three-point mountains are 6° and 12°, respectively. Note that the heights and

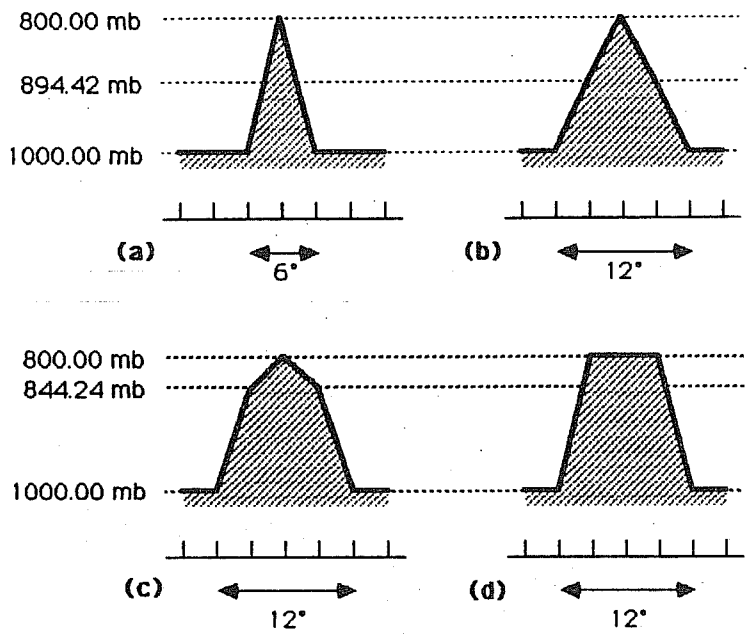

Fig. 7.2. Shapes of mountains used in the tests of Janjić (1989a): (a) single-point mountain; (b) three-point triangular mountain with the slopes linear in lnp; (c) three-point obelisk-shaped mountain; and, (d) three-point trapezoidal (elevated plateau) mountain. The heights of the mountain points and the base widths of the mountains are also indicated.

the slopes of the mountains chosen are rather modest compared to the examples of actual discretized topography given e.g., by Mesinger and Collins (1987). Nevertheless, difficulties may be expected with the spectral technique due to slow convergence of the Fourier series in the case of orography restricted to only several grid points.

In the finite-difference case irrespective of the shape of the mountain there were only hardly detectable errors for the no inversion profile. This should come as no surprise considering that this profile is linear in lnp, and that the same profile is assumed in (7.1) (e.g., Mesinger and Janjić 1985). Thus, the small discrepancies observed can be explained as the round-off errors. However, in the vertical columns with inversion, two-grid-interval noise appears, with the amplitude of slightly less than 2°K. This can be attributed to the averaging of temperature in (7.1).

In contrast to the finite-difference pressure gradient force error which is restricted to the points over the sloping terrain, the error of the spectral representation is spread over the horizontal domain. For this reason, the rms error is a more convenient measure of the pressure gradient force error than the grid point values.

The spectral rms pressure gradient force errors on the σ levels for the single-point mountain are shown in Fig. 7.3 (lightly shaded bars). The upper panel corresponds to the inversion, and the lower panel to the no inversion case. For comparison, the rms errors of the finite-difference method (cross hatched bars) are also displayed. Pressure gradient force errors of the spectral method shown in the figure are considerably larger than those of the finite-difference method, particularly in the no inversion case; in this case, as stated, the errors of the finite-difference method are hardly detectable.

In order to examine their spatial distribution, the pressure gradient force errors of the spectral method around the mountain point are plotted for the six lowest model levels in Fig. 7.4 (lightly shaded bars) for both inversion (left panel) and no inversion (right panel) cases. Going further up, the error patterns of levels 11 and 10 very much repeat themselves, switching from one to the other, depending on whether the vertical index is even or odd. For comparison, the finite-difference pressure gradient force error is also displayed (cross hatched bars) at the two points adjacent to the mountain point. It should be noted that the finite-difference errors are actually defined in between the mountain point and the two adjacent points. Thus, in the figure, they are shifted for half a grid distance away from their actual location.

Note that in the inversion case the amplitude of the spectral error wave packet is generally of the same order of magnitude as the errors of the finite-difference method.

The rms pressure gradient force errors obtained by Janjić for the trapezoidal shaped three-point mountain were slightly smaller but generally similar to those in Fig. 7.3. Errors for the three-point triangular and the obelisk-shaped mountain were significantly reduced but again clearly greater for the spectral than for the finite-difference method. Each time the errors of the finite-difference method in the no inversion case were at the round-off level as opposed to relatively large errors of the spectral method.

The four examples of small-scale mountains considered indicated that the σ-coordinate pressure gradient force errors of the spectral method can be large, and that the errors spread away from the mountains. In the rms sense, these errors were larger than the errors of the finite-difference method. In the inversion case, the amplitudes of the spectral error wave packets were generally of the same order of magnitude as the errors of the finite-difference method.

Contrary to the situation with the finite-difference method, the magnitude of the rms pressure gradient force error of the spectral method showed much less sensitivity to the absence of the inversion. Namely, the error of the latter remained relatively large, while the error of the former almost vanished.

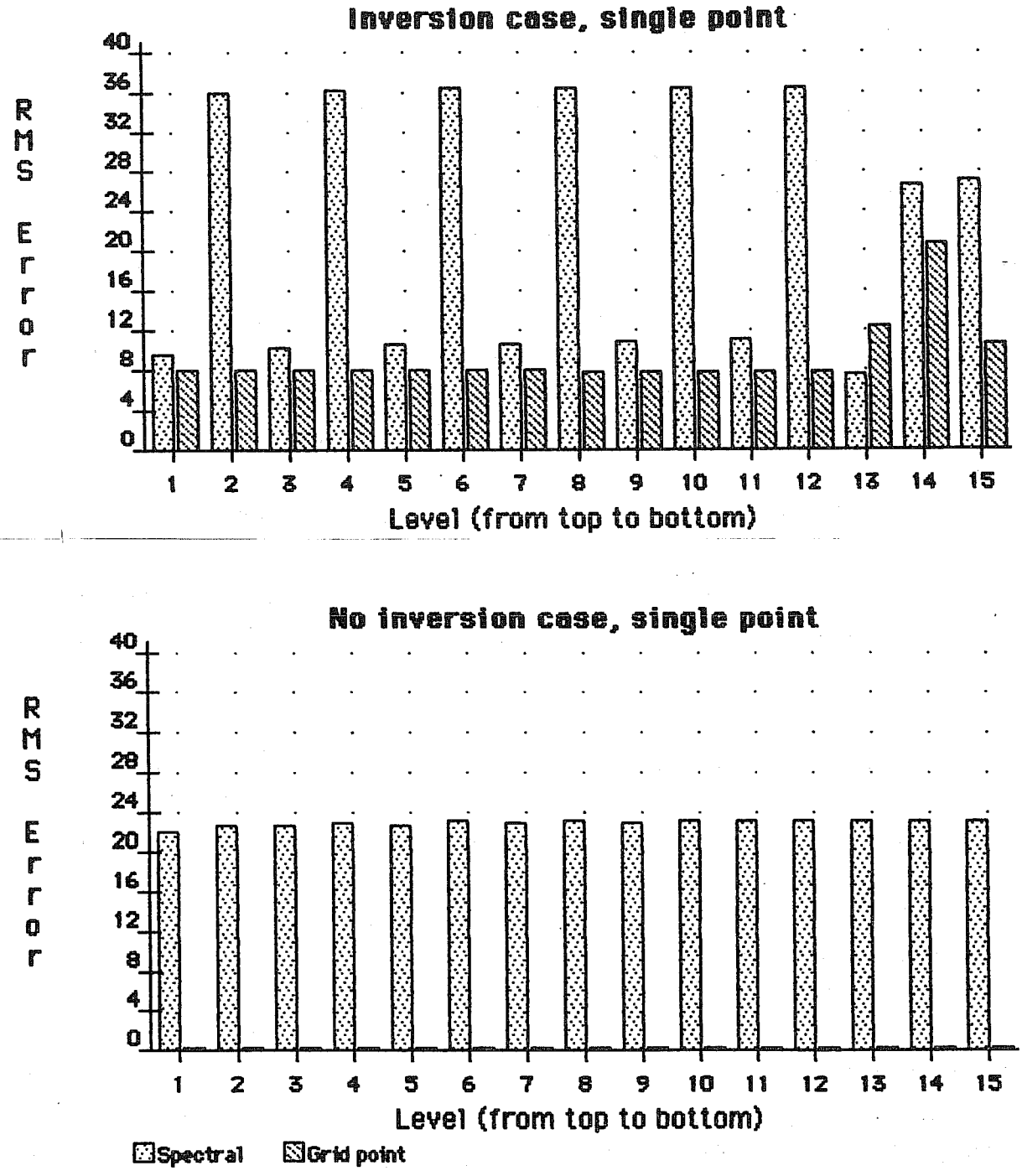

Fig. 7.3. The rms pressure gradient force errors corresponding to the single-grid point mountain for the inversion (upper panel) and no inversion (lower panel) cases (Janjić 1989a). The errors of the spectral and the finite-difference methods are represented by lightly shaded and cross-hatched bars, respectively. The plotted values are in units of geopotential.

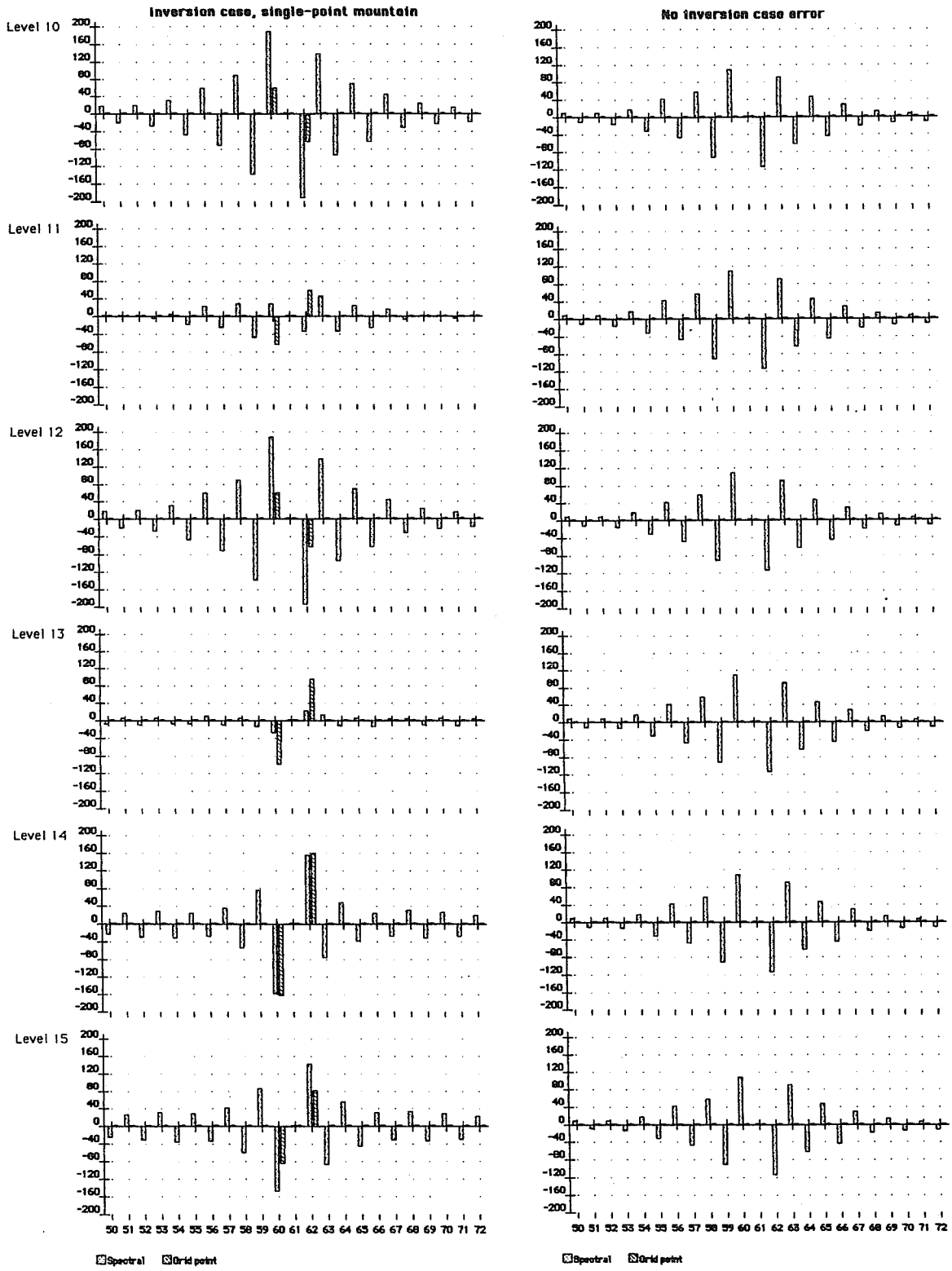

Fig. 7.4. Pressure gradient force error pattern around the mountain point at six lowest model levels for the spectral method (lightly shaded bars) and the finite-difference error (cross-hatched bars) for the "Inversion" (left panel) and the "No inversion" (right panel) cases (Janjić 1989a). The finite-difference error bars are shifted for half a grid distance in the direction away from the mountain from the actual error locations. The plotted values are in units of geopotential.

The experiments with varying the horizontal scale and the shape of the mountain, showed sensitivity of the spectral method to the steepness of the mountain. Generally, the steeper the mountain, the larger the pressure gradient force error. However, in the no inversion case, the rms errors of the generally steeper obelisk mountain were slightly smaller than those of the triangular mountain.

The pressure gradient force errors of the spectral method, as well as those of the finite-difference method, showed little sensitivity to changing from the single-point mountain to the trapezoidal three-point mountain. Note that the steepnesses of the slopes of these two mountains are the same. This suggests that the errors are less sensitive to the horizontal scale of the mountain than to its steepness.

Relatively large pressure gradient force errors of the spectral method observed in the no inversion case indicate that the mechanisms responsible for the error are different from those of the finite-difference σ-coordinate models.

As already pointed out, it seems natural to expect difficulties with spectral representation in the presence of small-scale topography because of slow convergence of the Fourier series. In this situation, in order to calculate the pressure gradient force in σ-coordinate spectral models, it may be advantageous to use the finite-difference technique on the finer grid used to eliminate aliasing.

8. *Conservation of integral quantities*

The work of Arakawa and Winninghoff in late 1960ies (Winninghoff 1968; Arakawa 1970) can probably be considered as marking the beginning of the studies of space discretization schemes for the primitive equations. In the course of two decades that have passed since that time a variety of properties of the discretized system have been looked into; see e.g., our earlier review paper on the present topic (Mesinger and Janjić 1987a). Some of the features frequently emphasized are those of the conservation of integral quantities, in particular of enstrophy in order to prevent a false energy cascade (Arakawa 1966, 1970; Arakawa and Lamb 1981; Janjić 1984); of the simulation of the geostrophic adjustment as a result of the choice of horizontal grid (Winninghoff 1968; Arakawa 1970); of the lack of aliasing; of the representation of mountains; and of a high Taylor-series type accuracy. Not all of these and other presumably desirable properties can however be achieved simultaneously and choices have to be made as to which of them if any will be sought. In doing this various authors have made different decisions. For example, a fully staggered

grid C or the semi-staggered grid E/B are needed from the point of view of the first two of the mentioned features and have repeatedly been chosen for these reasons. A nonstaggered A grid on the other hand has also more than once been chosen for its feature of being able to "accommodate high-order differencing with comparative ease" (Purser and Leslie 1988) even though it is highly undesirable from the former point of view.

This situation obviously reflects the difficulties of arriving at a convincing demonstration of the benefits of a given set of choices compared to other choices with a system as complex as the atmosphere. A general regard for a given approach is thus changing only as a result of the total body of evidence available and perhaps also as a result of the awareness of the existence of alternative techniques which eventually can be used.

In addition to points made so far which may contribute to assessments of this kind we wish to make two more points in the remainder of this lecture. One is to emphasize recently published results of Takacs (1988) concerning the effects of the conservation of enstrophy in horizontal advection and the choice of grid favorable from the point of view of geostrophic adjustment compared to those of a high Taylor-series accuracy and the high accuracy along with an a posteriori conservation technique. In Takacs' experiments two models were considered; one was an A-grid model with fourth-order accuracy and an optional a posteriori conservation of potential enstrophy. The other was a C grid model with fourth-order accuracy in horizontal advection terms only and an algebraic conservation of potential enstrophy. In the control experiment both model performed well at a relatively high $4° \times 5°$ resolution and gave similar results. Run at a course $8° \times 9°$ resolution the C grid model results did not change much, while those of the A grid model suffered a considerable degradation. Activation of the a posteriori enstrophy restoration feature of the A model achieved the enstrophy conservation but was of no help in alleviating the problems of the solution. It is pertinent in this respect to recall that the point of the enstrophy and energy conservation as introduced by Arakawa was not the conservation of these quantities in themselves but was the prevention of a false energy cascade through nonlinear interactions into small scales and degradation of the accuracy of the solution as a result. Filtering of smallest scales and an a posteriori restoration removes some of the resulting errors but not the erroneous energy cascade which appears to be the dominant problem of the course resolution experiment.

Since there is more than one important difference however between the two models compared by Takacs one cannot be certain as to which feature of the C

grid model to what extent contributed to the success of its course resolution experiment. But this is not critical from the practical point of view. Our remaining point is of the same nature in the sense that again the effect of a set of features is compared against that of another set. It consists of the examples of the results of the eta model compared against those of the U.S. operational regional model. As stated in the Introduction, a forecast of a surge of cold air and results of precipitation forecasts will be shown.

9. *Examples*

The two models we consider here are the so-called eta model of the U.S. National Meteorological Center, developed from the "minimum physics" HIBU (Hydrometeorological Institute and Belgrade University) model, and the U.S. operational regional model ("Nested Grid Model", NGM). They are different in three aspects of their space discretization schemes, as follows.

The eta model is using

- the eta vertical coordinate (Mesinger 1984) which permits step-like representation of mountains and quasi-horizontal coordinate surfaces;
- Arakawa E grid; and
- Janjić (1984) horizontal advection scheme which imposes a strict control on false energy cascade (e.g., Janjić and Mesinger 1984; Fig. 3.12).

The NGM is using

- the sigma vertical coordinate;
- Arakawa D grid; and
- Lax-Wendroff horizontal advection scheme (Phillips 1979; see also Mesinger and Arakawa 1976) with additional periodic filtering of 2 to $4\Delta x$ waves.

Both models include comprehensive physics packages (see, e.g., Janjić and Black 1987; Janjić 1989b, for the eta model physics; Tuccillo 1988 for the NGM physics). There are major differences in these; it is however believed that these differences do not have a significant impact on the first example to be shown (Subsection 9.1); and that their effect has been for the most part identified in the precipitation forecasts which will be discussed (Subsection 9.2) since along with the operational version of the NGM they have also been made with the NGM in which its Kuo convection scheme has been replaced by the Betts-Miller scheme (Betts 1986; Betts and Miller 1986) of the eta model. Reports on other comparisons of which perhaps most should also be largely independent of the differences in physical packages were made on earlier occasions (e.g., Black and Janjić 1988; Mesinger and Black 1989a, 1989b; Black

and Mesinger 1989a, 1989b).

Still another difference to be aware of is the treatment of the boundary conditions. NGM is a two-way triply nested model with its highest resolution domain (e.g., Hoke et al. 1985) perhaps slightly larger than that of the eta model. Lateral boundary conditions of the eta model are prescribed in a one-way mode using the results of the NMC global medium-range forecast (MRF) model. They are however taken from the 12 hours earlier MRF (aviation) run in order to simulate an operational situation in which the short-range model is run prior to the medium-range one.

9.1 *The cold air outbreak of February 1989*

A severe failure of the U.S. operational regional model took place in early February 1989. Following accumulation of an exceptionally cold air over northwestern North America, with values of pressure reduced to sea level among the several highest on record, a major cold air outbreak occurred along the eastern slopes of Rockies. The operational model however developed a low in the lee of Rockies which inhibited the southward movement of the cold air. This is shown in Fig. 9.1.1. NMC analysis for 1200 UTC 2 February is shown in its upper left hand panel. In this analysis for example the 1020 mb isobar is seen reaching as far south as the central Oklahoma. In the NGM 36 h forecast valid at that time, lower left hand panel, the 1020 isobar is much further to the north barely crossing the border from the North into the northwestern South Dakota. Run from the same initial condition and with about the same horizontal and vertical resolution the eta model is giving a much more accurate forecast, shown in the upper right hand panel of the figure.

The reduction to sea level usually used in the eta post-processing code and also to display the forecast in the figure is the so-called horizontal (or "relaxation temperature") reduction. It is based on underground virtual temperatures computed in each model layer which contains mountains by solving the Laplace equation with virtual temperatures next to the sides of mountains as boundary conditions. It is our impression that this horizontal reduction method although very different from the one used in synoptic practice nevertheless results in sea level pressure maps which are generally more like the analyzed maps than those obtained by a "standard" reduction based on temperatures immediately above ground and a lapse rate of 0.0065 K m^{-1}. It is perhaps the optimal reduction method possible since it involves replacing the mountain by an atmosphere which is most like the air around the mountain at a given time and place. But with surface air as cold as in the situation of Fig. 9.1.1 the reduction based on temperatures immediately above ground does give a sea level pressure

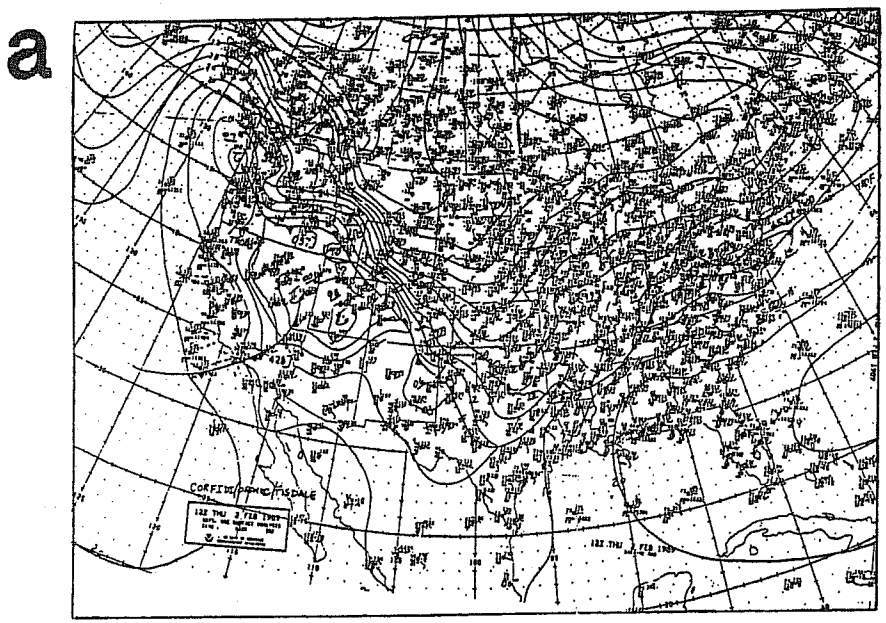

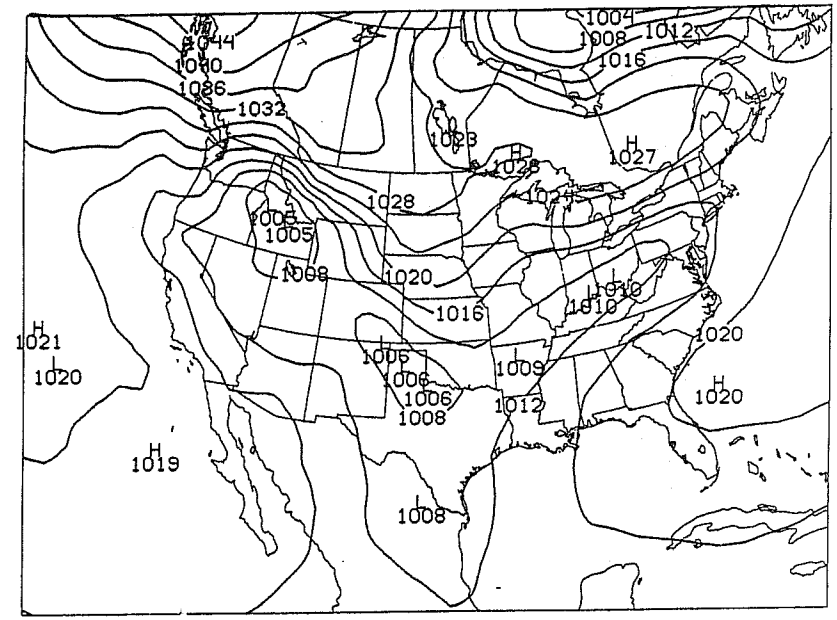

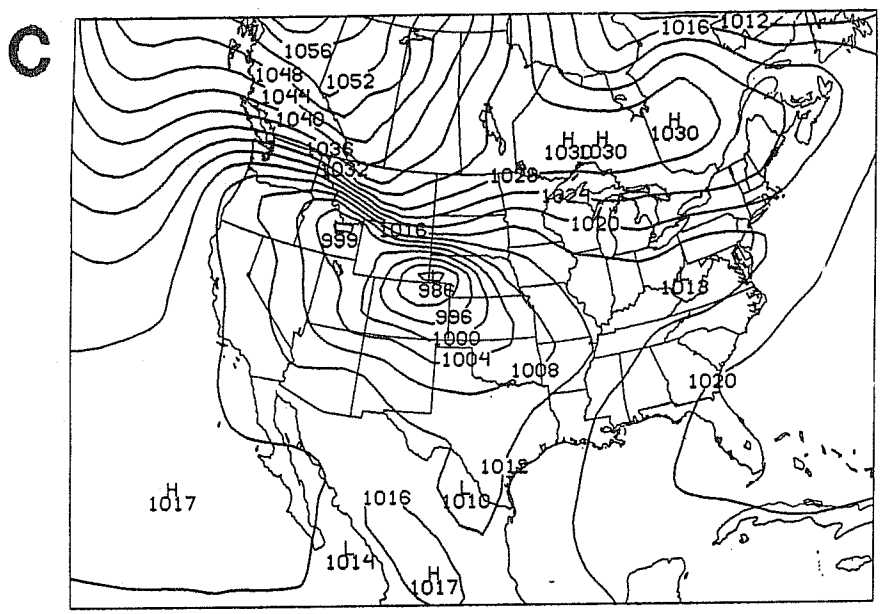

Fig. 9.1.1. Mean sea level pressure (mb) for 1200 UTC 2 February 1989: (a) NMC analysis; (b) 36 h eta model forecast; (c) 36 h NGM forecast.

field which is more like the analyzed field seen in panel (a) than the one of panel (b). Namely, with standard reduction, a band of very closely packed isobars appears across Montana and Wyoming very much in the manner of panel (a) and the 1020 isobar is obtained several hundred kilometers further south than in panel (b), about half-way between its positions in these two panels.

Experiments performed with the eta model run in the sigma mode and with mountains interpolated from the NGM mountains indicate that the geometry of the eta model mountains, presumably their steepness, was a major contributor to the successful eta result in this case.

9.2 *Precipitation forecasts and scores*

While successful forecasts for difficult situations of special interest are most gratifying it is only through examination and if possible statistical analysis of a large sample that one gains confidence regarding the overall performance of a model including its discretization schemes. We have from this point of view paid most attention to precipitation forecasts for a number of reasons. One is that weather is of course the ultimate objective of weather forecasting and precipitation can hardly be surpassed in terms of priority from that point of view. Another is that precipitation in particular of convective type tends to occur on a rather small scale and thus seems to be the element to improve upon through development of limited area models such as the eta model. Still another of our reasons is that increasing the accuracy of precipitation forecasts has proven to be notoriously difficult ("quantitative precipitation forecasts remain elusive" states a recent yearly report of an elite laboratory). Indeed, numerical values of precipitation scores are low and if one believes to have improved on relevant components of a prediction model without neglecting its other relevant components one should expect to see the improvements result in increased precipitation scores.

The score we here have in mind is the threat score (e.g., Anthes 1983)

$$\frac{CF}{F+O-CF} \qquad (9.2.1)$$

where CF is the correctly forecast, F the total forecast and O the observed area, respectively, of the accumulated precipitation above a given amount. Threat scores, and bias scores, F/O, can routinely be obtained at NMC for precipitation accumulated over 24-hour intervals, verifying at 1200 UTC, and averaged over grid boxes of the so-called Limited Fine Mesh (LFM) model (190° × 190° at 60° latitude on stereographic projection). Scores are calculated for about the eastern two thirds of the continental United States, and for the categories of

precipitation amounts equal to and greater than 0.01, 0.25, 0.50, 0.75, 1.00, 1.25, 1.50, 1.75, 2.00, 2,50, 3.00, 3.50 and 4.00 inches in 24 hours.

The period particularly suitable for the present purpose was that of 1200 UTC 16 June - 5 July 1989 since during that time (a) there was no change in the semi-operationally twice-daily run version of the eta model and (b) results of the NGM run as stated with the Betts-Miller convection scheme of the eta model were also available. Condition (a) was not fulfilled prior to 16 June and the condition (b) not after 5 July so that the considered 20-day verification period is the longest for which both of these conditions are satisfied and the three-way model comparison possible.

Weather during 16 June - 5 July 1989 over the eastern two thirds of continental United States was perhaps exceptionally wet so that for example on two of these 20 verification periods average LFM grid box precipitation of over 4 inches in 24 hours was recorded, and only on 5 periods maximum precipitation was less than 1.75 inches in 24 hours. This was largely due to tropical storm Allison which slowly approached the Texas-Louisiana coastline at about the middle of this period and then although its center moved over land remained near the Gulf Coast for about four days causing heavy rains and flooding in regions around the Texas-Louisiana border.

Since forecasting correctly the location of the precipitation maximum in such and other cases is of special interest and not something prediction models as of yet are famous for we have searched the considered sample for cases in which the models retained skill greater than zero through the highest category of the "observed" precipitation. One should note that positive skill can be retained through the highest category as a result of model's tendency to overforecast the amounts of precipitation but this for the most part was not happening within the considered sample as we shall document later on. Each of the three models has been run out to 48 hours starting every 0000 and 1200 UTC within the considered period and the 24 hours prior to it. Two forecasts, for all of the models, were however not accessible to the verification code because of archiving problems; the sample thus consisted of 39 forecasts of each of the three models. We should in addition note that the forecasts starting at 1200 UTC were each verified for two of their forecast periods, 00-24 and 24-48 h; and those starting at 0000 UTC once, for their 12-36 h forecasts. The two forecasts missing were forecasts starting at 0000 UTC, verifying once. Thus, within the 20 verification periods, we have verifications for 58 accumulated precipitation forecasts, for each of the three models.

In this sample of 58 verifications, the NGM retained skill greater than zero through all of the precipitation categories observed 2 times; NGM with the Betts-Miller convection (NGMx, for experimental) 12 times; and the eta model 14 times.

We want to discuss two points in connection with these numbers. One is the extent to which they are a result of the biases of the models for heavier precipitation amounts. For the NGM the effect is large. Its Kuo scheme has a severe bias problem in the sense of being deficient in heavier precipitation amounts. For example, of the 58 24-hour verifications it has never produced LFM grid box amounts of 3.5 inches and greater even though the amounts of 4 inches and greater have been observed at 2 verification periods, that is, for 6 verifications. With the Betts-Miller scheme NGM's precipitation patterns are much more concentrated (see also Plummer et al. 1989) as are those of the eta model, and the ability to retain positive skill through all of the categories observed is much improved.

For an assessment now of a possible difference between the two models using the Betts-Miller scheme in the tendency to benefit from overforecasting the precipitation amounts we have looked at the bias scores for their 12 and 14 realizations of positive skill. One should note that in this way we are looking at a sample from which occurrences of zero bias score have been removed so that an unbiased model, with average bias score equal to one, should have a bias greater than one for a sample remaining after this elimination. Indeed, the ratios of forecast and observed LFM grid boxes ("points") for the 12 realizations of the NGMx model were

$$\frac{2}{1}, \frac{2}{2}, \frac{1}{1}, \frac{2}{1}, \frac{10}{2}, \frac{3}{3}, \frac{5}{3}, \frac{2}{2}, \frac{2}{1}, \frac{5}{1}, \frac{5}{1}, \frac{5}{1}, \tag{9.2.2}$$

which gives an average over the 12 values of 2.64; and the ratios for the 14 realizations of the eta model

$$\frac{2}{2}, \frac{2}{1}, \frac{1}{1}, \frac{3}{1}, \frac{3}{1}, \frac{4}{2}, \frac{3}{2}, \frac{13}{2}, \frac{1}{1}, \frac{2}{1}, \frac{2}{1}, \frac{2}{3}, \frac{4}{3}, \frac{3}{3}, \tag{9.2.3}$$

with an average of 1.96. If, on the other hand, the average value of the bias score for these realizations is calculated by dividing the total number of forecast points by the total number of observed points, the values obtained are 2.32 and 1.88, respectively. In any case, the numbers looked at above do not support a possible suspicion that the slightly higher number of realizations of the eta model, 14 versus 12, came as a result of overforecasting the highest

precipitation amounts. Both models, in fact, underforecast the highest precipitation amounts, the eta model somewhat more than the NGMx, as one can verify by calculating the averages over all 58 verifications. One obtains averages of 0.55 and 0.47 for the NGMx and for the eta model, respectively, using the former of the two calculation methods.

The second point we want to discuss concerns the distribution of the cases of positive skill at the highest observed category. We here restrict our attention to the eta model only. This distribution, along with the maximum categories observed, is displayed in Table 1.

Table 1. Forecast periods within the sample of 58 verifications for which the eta model had skill at the highest observed precipitation category, and values of these highest categories

Verification date	Forecast period			Highest category observed
16 June	00-24 h			3.00 inches/24 h
17 June			24-48 h	2.00 inches/24 h
24 June	00-24 h	12-36 h	24-48 h	1.75 inches/24 h
26 June	00-24 h	12-36 h	24-48 h	1.50 inches/24 h
27 June	00-24 h	12-36 h		4.00 inches/24 h
29 June			24-48 h	2.50 inches/24 h
1 July	00-24 h	12-36 h	24-48 h	2.00 inches/24 h

A remarkable feature of this table is the tendency of the 14 realizations to occur for the same verification periods, that is, irrespective of the initial times. At three of the 18 periods when this was possible positive skill at the highest observed category was present for all three forecast periods; and of the remaining 5 realizations 2 have once more occurred for the same verification period. Given the overall probability of a realization in a given verification, of 14/58, and the total number of 14 realizations, probability of such clustering by chance is less than 3/10,000. We see this as giving strong support for the ability of the model to forecast the location of the precipitation maxima, not by chance, but because of model's capability to handle certain situations given its present resolution, numerical schemes and physics. Perhaps, with improvements in each or in some of these components, the repertoire of model's heavy precipitation situations should increase, so that more of them become predictable.

We shall show examples of precipitation forecasts for two of the verification periods of Table 1. One are the three forecasts verifying at 1200 UTC 27 June.

They are shown in the upper right hand and in the two lower panels of Fig. 9.2.1. Analyzed precipitation verifying at the same time is shown in the upper left hand panel of the same figure. This is the first verification period for which the center of precipitation due to tropical storm Allison was located over land and is also the period of Table 1 with the highest observed precipitation. Note that the ratios (9.2.3) of forecast and observed LFM points at the maximum category are written in the same order as the forecast periods of Table 1; one can thus locate in this sequence the ratios of forecast and observed LFM points of 1/1 and 2/1 of the 00-24 and 12-36 h forecasts shown in the figure, respectively. Thus, in both cases the model has correctly forecast the single LFM grid box with precipitation over 4 inches in 24 hours; and in the 00-24 h forecast this was at the same time the only point of that precipitation category forecast.

Following landfall the Allison precipitation center moved east and was located over southern central Louisiana at the next verification time. Subsequently while reducing its intensity it moved back to the Texas-Louisiana border and at 1200 UTC 29 June was located north of its position seen in Fig. 9.2.1. During the following 24 hours while weakening again a little it moved back south to about the same position as the one of the 27 June. Finally during still another 24 hours the center moved north-northeast so that at 1200 UTC 1 July it was located at the Arkansas-Louisiana border. The three forecasts verifying at that time are our second example shown in Fig. 9.2.2 in the same layout as the one of the preceding figure. Note that this is the first verification time for which the precipitation center has moved deeper inland after staying at or close to the Gulf Coast for the preceding four to five days and that in all three forecasts this movement was predicted.

We finally show in Fig. 9.2.3 the threat scores for the three models averaged for all 58 verifications. "Averaging" is performed by adding all the correctly forecast, total forecast and observed points prior to inserting the values into (9.2.1). Note that in this way incorrectly forecast points at categories above that of the maximum observed penalize the values of the average score which is of course desirable but would not happen if the threat scores were first calculated for individual verifications and then averaged over categories for which precipitation was observed and individual values thus available. Comparison of the eta and the NGM results is shown in the upper panel of the figure. The eta model is seen to lose the lightest precipitation category of .01 inches and greater. Its bias score (not shown) at this category for the considered sample was only .74, compared to 1.10 for the NGM. The next higher category of .25 inches and greater is about a tie. The eta models wins all the

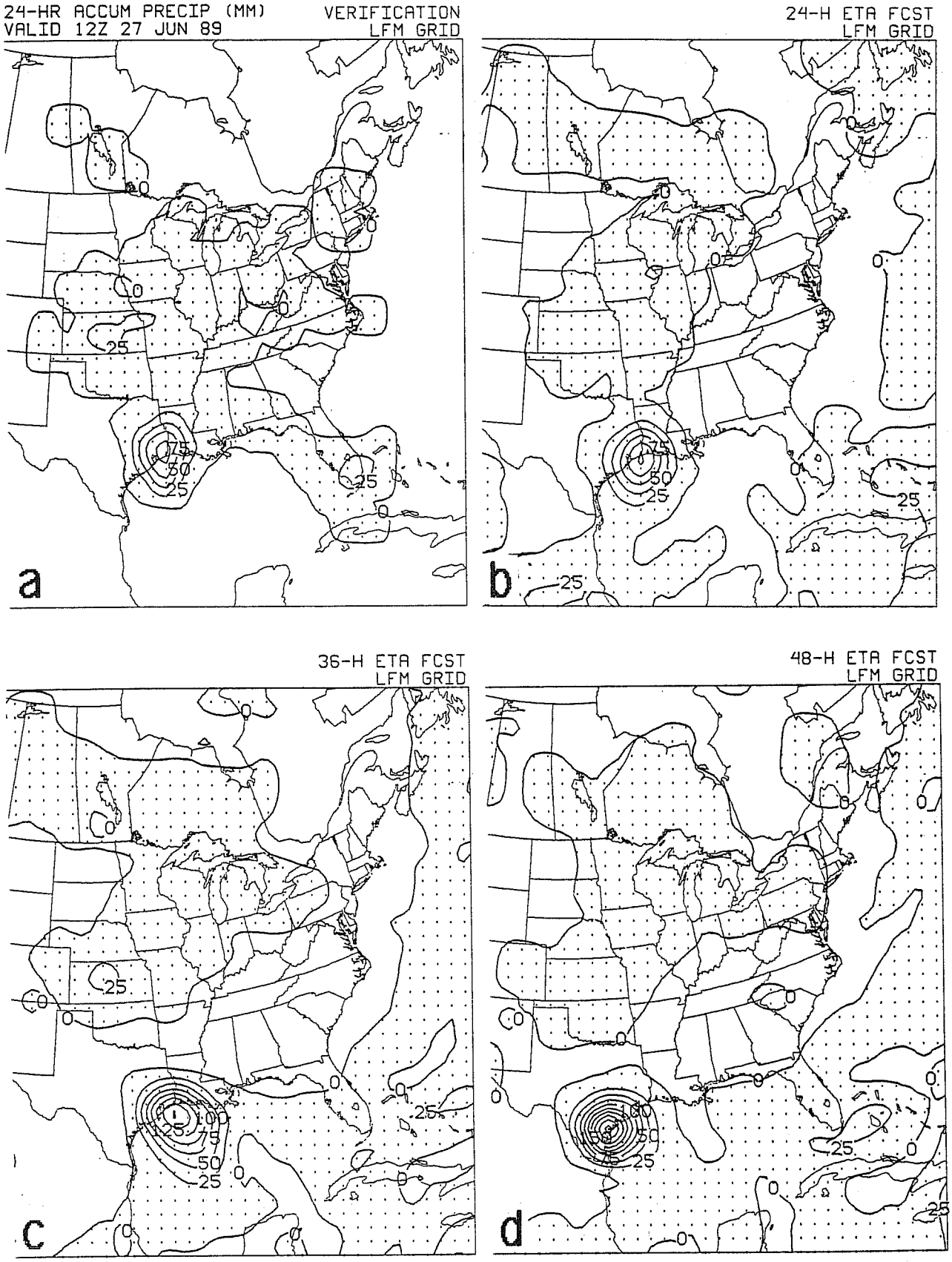

Fig. 9.2.1. 24-h accumulated precipitation, in millimeters, verifying at 1200 UTC 27 June 1989: (a) NMC analysis; (b) 00-24 h, (c) 12-36 h, and (d) 24-48 h eta model forecast, respectively.

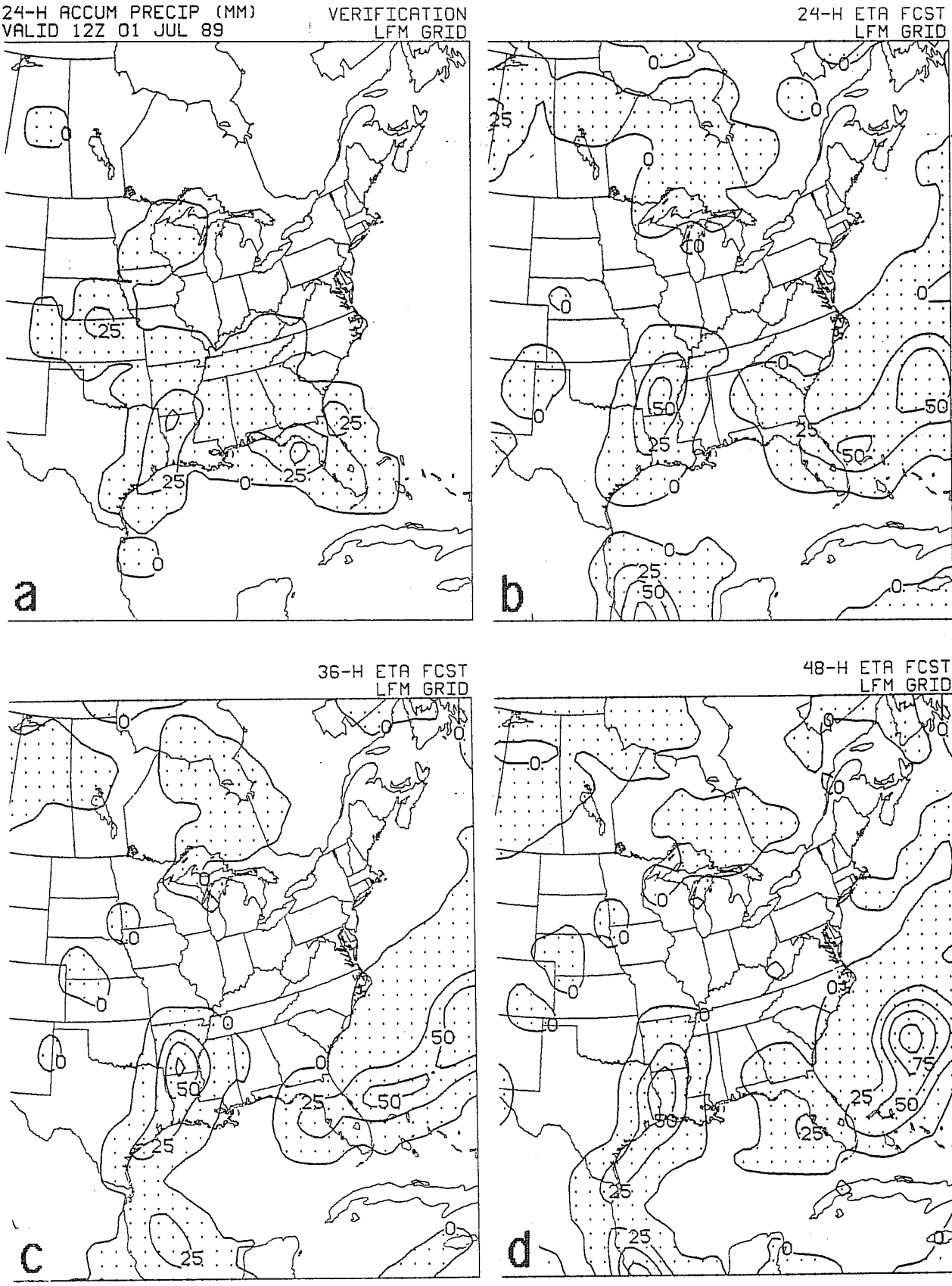

Fig. 9.2.2. 24-h accumulated precipitation, in millimeters, verifying at 1200 UTC 1 July 1989: (a) NMC analysis; (b) 00-24 h, (c) 12-36 h, and (d) 24-48 h eta model forecast, respectively.

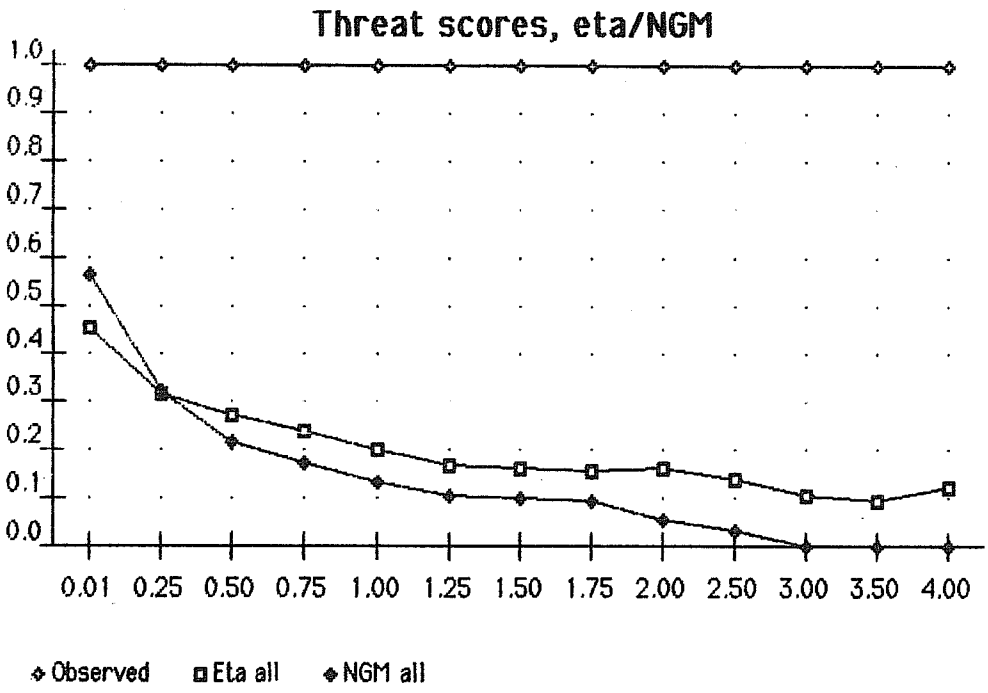

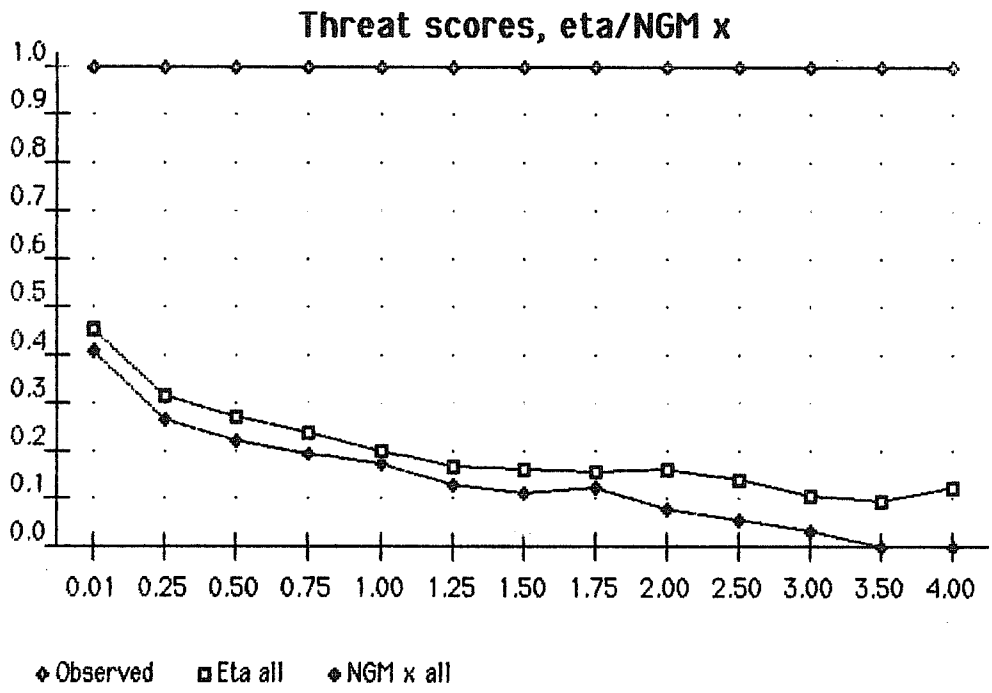

Fig. 9.2.3. Threat scores for various precipitation categories, in inches, of 24-hour accumulated precipitation of the eta model, NGM, and NGMx (NGM with Betts-Miller convection scheme) for 58 forecasts verifying every 1200 UTC within the period 16 June - 5 July 1989. See text for additional details. Eta model and NGM, upper panel; eta model and NGMx, lower panel.

remaining categories, more and more convincingly as the amounts are greater. At the higher categories, as stated earlier, it is the NGM Kuo scheme that has a severe bias problem. For example, at 2.00 inches and greater NGM had the bias score of only .62 compared to 1.11 for the eta model.

Regarding the effect of differences in space discretizations however of more interest is the comparison between the eta model and the NGMx, shown in the lower panel of the figure. With the same convection scheme of these two models the eta model wins all of the categories, perhaps about equally convincingly for the light and for the intense precipitation. The bias problem of the eta model for the light precipitation categories is even more severe for the NGMx, indicating that this problem is a feature of the convection scheme and not of the space discretization of the models. Further work aimed at refining the Betts-Miller scheme of the eta model and its related parameterizations with respect to the extent of light precipitation is in progress at the National Meteorological Center and is expected to be reported on at another occasion.

We see the results of the lower panel of Fig. 9.2.3 as yet another addition to the body of evidence in favor of the space discretization features of the eta model compared to those of the control model as given in the introductory part of the section. At the same time, along with data of Table 1 we find them a welcome encouragement from the point of view of progress in the predictability of precipitation patterns, a long-standing issue of concern in numerical weather prediction.

10. Summary

Rather than review the basic properties of space discretization schemes for the primitive equations we have attempted in this lecture to outline recently completed work and work in progress in this field, emphasizing motivations for various efforts. We have also commented on outstanding problems which in our opinion if and when resolved could lead to further progress.

Perhaps most numerous of recent and present efforts are those aimed at increasing the efficiency of space discretizations through the development and use of semi-Lagrangian schemes. They are addressed not only at increasing the time steps but also at the pole problem of the global finite-difference models. Still another objective of this but also of other work is to increase the ability of models to generate and maintain sharp features in predicted fields. Extensive testing of the step-mountain approach in finite-difference models is in progress at NMC with perhaps very encouraging results as reported to some extent in this lecture.

We have stressed a number of challenging problems on which little work has been and is being done. One is the inconsistency between methods used for space discretization and those used for physical parameterization schemes. Another is the inefficiency of global latitude-longitude finite-difference representation not only because of the CFL time step condition but also from the point of view of redundant resolution in zonal direction in extratropical latitudes. Still another is the treatment of mountains in spectral models.

Reflecting back on the past two or three decades of the development of methods for space discretization in weather prediction we find as perhaps remarkable the degree to which this development was in many ways leading that of numerical analysis and other applied fluid dynamics fields. Thus, fundamental advances have been made as part of the numerical modeling work in meteorology and some have found its way into other computational fluid dynamics fields. Outstanding examples include the discovery and the explanation of nonlinear instability by Phillips; the Arakawa approach in designing finite-difference schemes which maintain chosen integral properties of the continuous equations, or reproduce their other features of physical importance; several major steps in the development of the present global spectral transform method in particular the introduction of the transform itself by Eliasen, Machenhauer and Rasmussen independently of Orszag; and the discovery of the semi-Lagrangian schemes by Robert. But it may be that a turn has come for a method developed outside meteorology, the piecewise parabolic method, to becomes increasingly used in weather prediction enabling further and perhaps unexpected progress.

Acknowledgments. Collaboration of Tom Black of the U.S. National Meteorological Center has been essential in obtaining the results reported in Section 9 of this lecture. John Ward of the same Center has written the precipitation verification code and has implemented the archiving system indespensable for processing of the large three-model sample dealt with here. Support and encouragement of William Bonner, Director, and Eugenia Kalnay, Chief of the Development Division of the Center was vital for the succcess of a project as comprehensive as the substantial part of the development as well as the semi-operational implementation of the eta model and is gratefully acknowledged. Our work on some of the material presented has been partly supported by the Science Association of Serbia; and by the Serbian Academy of Sciences and Arts, Belgrade.

References

Anthes, R. A., 1983: Regional models of the atmosphere in middle latitudes. Mon. Wea. Rev., **111**, 1306-1335.

Arakawa, A., 1966: Computational design for long-term numerical integration of equations of fluid motion: Two dimensional incompressible flow. Part I. J. Comput. Phys., **1**, 119-143.

Arakawa, A., 1970: Numerical simulation of large-scale atmospheric motions. Numerical Solution of Field Problems in Continuum Physics, Vol. 2. SIAM-AMS Proceedings, G. Birkhoff and S. Varga, Eds., Amer. Math. Soc., 24-40.

Arakawa, A. and V. R. Lamb, 1981: A potential enstrophy and energy conserving scheme for the shallow water equations. Mon. Wea. Rev., **109**, 18-36.

Bates, J. R., and A. McDonald, 1982: Multiply-upstream, semi-Lagrangian advective schemes: analysis and application to a multi-level primitive equation model. Mon. Wea. Rev., **110**, 1831-1842.

Bates, J. R., F. H. M. Semazzi, R. W. Higgins and S. R. M. Barros, 1989: Integration of the shallow water equations on the sphere using a vector semi-Lagrangian scheme with a multigrid solver. Subm. to Mon. Wea. Rev.

Betts, A. K., 1986: A new convective adjustment scheme. Part I: Observational and theoretical basis. Quart. J. Roy. Meteor. Soc., **112**, 677-691.

Betts, A. K., and M. J. Miller, 1986: A new convective adjustment scheme. Part II: Single column tests using GATE wave, BOMEX and arctic air-mass data sets. Quart. J. Roy. Meteor. Soc., **112**, 693-709.

Black, T. L., and Z. I. Janjić, 1988: Preliminary forecast results from a step-mountain eta coordinate regional model. Preprints, Eighth Conf. Numerical Weather Prediction, Baltimore, Amer. Meteor. Soc., 442-447. [Boston, MA 02108.]

Black, T. L., and F. Mesinger, 1989a: Forecast performance of NMC's eta coordinate regional model. Preprints, Twelfth Conf. Weather Analysis and Forecasting, Monterey, CA, 2-6 October 1989; Amer. Meteor. Soc., (in press). [Boston, MA 02108.]

Black, T. L., and F. Mesinger, 1989b: Forecasting for the South American Region using an eta coordinate regional model. Preprints, Third Int. Conf. Southern Hemisphere Meteorology and Oceanography, Buenos Aires, 13-17 November 1989; Amer. Meteor. Soc., (in press). [Boston, MA 02108.]

Bleck, R., and G. Peng, 1989: Numerical model errors affecting the simulation of lee cyclogenesis. Preprints, Int. Conf. Mountain Meteor. and ALPEX, Garmisch-Partenkirchen, 53-54. [Available from Inst. Physik Atmos., DLR, D-8031 Oberpfaffenhofen, FRG.]

Bott, A., 1989: A positive definite advection scheme obtained by nonlinear renormalization of the advective fluxes. Mon. Wea. Rev., **117**, 1006-1015.

Bourke, W., 1974: A multi-level spectral model. I. Formulation and hemispheric integrations. Mon. Wea. Rev., **102**, 687-701.

Browning, G. L., J. J. Hack and P. N. Swarztrauber, 1989: A comparison of three numerical methods for solving differential equations on the sphere. Mon. Wea. Rev., **117**, 1058-1075.

Carpenter, R. L., Jr., K. K. Droegemeier, P. W. Woodward and C. E. Hane, 1989: Application of the piecewise parabolic method (PPM) to meteorological modeling. Mon. Wea. Rev., **117**, (in press).

Colella, P., and P. R. Woodward, 1984: The piecewise parabolic method (PPM) for gas-dynamical simulations. J. Comput. Phys., **54**, 174-201.

Courtier, P., and J.-F. Geleyn, 1988: A global numerical weather prediction model with variable resolution: Application to the shallow water equations. Quart. J. Roy. Meteor. Soc., **114**, 1321-1346.

Droegemeier, K. K., and R. B. Wilhelmson, 1987: Numerical simulations of thunderstorm outflow dynamics. Part I: Outflow sensitivity experiments and turbulence dynamics. J. Atmos. Sci., **44**, 1180-1210.

ECMWF, 1984: Numerical Methods for Weather Prediction. Seminar 1983, ECMWF, Reading, Shinfield Park, U.K., 290+300 pp.

ECMWF, 1988: Techniques for Horizontal Discretization in Numerical Weather Prediction Models. Workshop 1987, ECMWF, Shinfield Park, Reading, U.K., 378 pp.

Egger, J., 1971: Mindestgrösse von Gebirgen und Konvektionsgebieten, die in den Modellen der numerischen Vorhersage berücksichtigt werden können. Beitr. Phys. Atmos., **44**, 245-271.

Farge, M., and R. Sadourny, 1989: Wave-vortex dynamics in rotating shallow water. J. Fluid Mech., (in press).

Godunov, S. K., 1959: Finite difference methods for numerical computation of discontinuous solutions of the equations of fluid dynamics. Mat. Sb., **4**, 271-306. (Cornell Aeronautical Lab. Transl.)

Hoke, J. E., N. A. Phillips, G. J. DiMego and D. G. Deaven, 1985: NMC's regional analysis and forecast system - results from the first year of daily, real-time forecasting. Preprints, Seventh Conf. Numerical Weather Prediction, Montreal, Amer. Meteor. Soc., 444-451. [Boston, MA 02108.]

Hsu, Y.-J., 1988: Numerical modeling of the atmosphere with an isentropic vertical coordinate. Ph. D. Thesis, Dept. Meteor. Univ. California, Los Angeles, CA 90024.

Janjić, Z. I., 1984: Non-linear advection schemes and energy cascade on semi-staggered grids. Mon. Wea. Rev., **112**, 1234-1245.

Janjić, Z. I., 1989a: On the pressure gradient force error in σ-coordinate spectral models. Mon. Wea. Rev., **117**, 2285-2292.

Janjić, Z. I., 1989b: The step-mountain coordinate: physical package. Mon. Wea. Rev., **117**, (in press).

Janjić, Z. I., and T. L. Black, 1987: Physical package for the step-mountain, eta coordinate model. Res. Activ. Atmos. Oceanic Modelling, No. 10, 5.24-5.26.

Janjić, Z. I., and F. Mesinger, 1984: Finite difference methods for the shallow water equations on various horizontal grids. Numerical Methods for Weather Prediction. Seminar 1983, ECMWF, Reading, Shinfield Park, U.K., 29-101.

Janjić, Z. I., and F. Mesinger, 1989: Response to small-scale forcing on two staggered grids used in finite-difference models of the atmosphere. Quart. J. Roy. Meteor. Soc., **115**, 1167-1176.

Janjić, Z. I., F. Mesinger and T. L. Black, 1988: Horizontal discretization and forcing. Workshop on Numerical Techniques for the Horizontal Discretization in Numerical Weather Prediction Models. Workshop 1987, ECMWF, Shinfield Park, Reading, U.K., 207-227.

Janjić, Z., and A. Wiin-Nielsen, 1977: On geostrophic adjustment and numerical procedures in a rotating fluid. J. Atmos. Sci., **34**, 297-310.

McDonald, A., and J. R. Bates, 1989: Semi-Lagrangian integration of a gridpoint shallow water model on the sphere. Mon. Wea. Rev., **117**, 130-137.

Mesinger, F., 1982: On the convergence and error problems of the calculation of the pressure gradient force in sigma coordinate models. Geophys. Astrophys. Fluid. Dyn., **19**, 105-117.

Mesinger, F., 1984: A blocking technique for representation of mountains in atmospheric models. Riv. Meteor. Aeronautica, **44**, 195-202.

Mesinger, F., 1985: The sigma system problem. Preprints, Seventh Conf. Numerical Weather Prediction, Montreal, Amer. Meteor. Soc., 340-347. [Boston, MA 02108.]

Mesinger, F., and A. Arakawa., 1976: Numerical Methods used in Atmospheric Models. GARP Publ. Ser., No. 17, Vol. I, WMO, Geneva, 64 pp. [Pub. WMO/ICSU, Case Postale No. 2300, CH-1211 Geneva 20, Switzerland.]

Mesinger, F., and T. L. Black, 1989a: Verification tests of the eta model, October-November 1988. NOAA/NWS National Meteorological Center, Office Note No. 355, 47 pp.

Mesinger, F., and T. L. Black, 1989b: A mountain-induced secondary development associated with severe weather east of Appalachians. Preprints, Int. Conf. Mountain Meteorology and ALPEX, Garmisch-Partenkirchen, F.R.G., 5-9 June 1989; DLR-Institute for Atmospheric Physics, Oberpfaffenhofen, 55-58.

Mesinger, F., and W. G. Collins, 1987: Review of the representation of mountains in numerical weather prediction models. Observation, Theory and Modelling of Orographic Effects, Seminar/workshop 1986, Vol. 2, ECMWF, Shinfield Park, Reading, U.K., 1-28.

Mesinger, F., and Z. I. Janjić, 1985: Problems and numerical methods of the incorporation of mountains in atmospheric models. Large-scale Computations in Fluid Mechanics, Part 2. Lect. Appl. Math., Vol. 22, Amer. Math. Soc., 81-120.

Mesinger, F., and Z. I. Janjić, 1987a: Numerical Methods in NWP models. Short- and Medium- Range Numerical Weather Prediction: Collection of Papers Presented at the WMO/IUGG NWP Symposium, Tokyo, 4-8 August 1986, Special Volume of J. Meteor. Soc. Japan, Ed. T. Matsuno, 215-222.

Mesinger, F., and Z. I. Janjić, 1987b: Numerical techniques for the representation of mountains in atmospheric models. Observation, Theory and Modelling of Orographic Effects, Seminar/workshop 1986, Vol. 2, ECMWF, Shinfield Park, Reading, U.K., 29-80.

Mesinger, F., Z. I. Janjić, S. Ničković, D. Gavrilov and D. G. Deaven, 1988: The step-mountain coordinate: model description and performance for cases of Alpine lee cyclogenesis and for a case of Appalachian redevelopment. Mon. Wea. Rev., **116**, 1493-1518.

Phillips, N. A., 1979: The Nested Grid Model. NOAA Tech. Rep. NWS 22, National Weather Service, Silver Spring, MD., 80 pp.

Plummer, D. W., T. L. Black, N. A. Phillips and J. E. Hoke, 1989: Tests of the Betts-Miller convective parameterization in the Nested Grid Model. Research Highlights of the NMC Development Division: 1987-1988. U.S. Dept. Commerce, NOAA, National Weather Service, 23-32.

Priestley, A., 1988: The use of a characteristics based scheme for the 2-D shallow water equations. Techniques for Horizontal Discretization in Numerical Weather Prediction Models. Workshop 1987, ECMWF, Shinfield Park, Reading, U.K., 157-185.

Purser, R. J., 1988a: Degradation of numerical differencing caused by Fourier filtering at high latitudes. Mon. Wea. Rev., **116**, 1057-1066.

Purser, R. J., 1988b: Accurate numerical differencing near a polar singularity of a skipped grid. Mon. Wea. Rev., **116**, 1067-1076.

Purser, R. J., and L. M. Leslie, 1988: A semi-implicit, semi-Lagrangian finite-difference scheme using high-order spatial differencing on a nonstaggered grid. Mon. Wea. Rev., **116**, 2069-2080.

Rančić, M., and S. Ničković, S., 1988: Numerical testing of E-grid horizontal advection schemes on the hemisphere. Contrib. Atmos. Phys., **61**, 265-273.

Rančić, M., and G. Sindić, 1989: Noninterpolating semi-Lagrangian advection scheme with minimized dissipation and dispersion errors. Mon. Wea. Rev., **117**, (in press).

Robert, A., 1981: A stable numerical integration scheme for the primitive meteorological equations. Atmos.-Ocean, **19**, 35-46.

Robert, A., 1982: A semi-Lagrangian and semi-implicit numerical integration scheme for the primitive meteorological equations. J. Meteor. Soc. Japan, **60**, 319-324.

Sadourny, R., 1972: Conservative finite-difference approximations of the primitive equations on quasi-uniform spherical grids. Mon. Wea. Rev., **100**, 136-144.

Sadourny, R., 1975: Compressible model flows on the sphere. J. Atmos. Sci., **32**, 2103-2110.

Schmidt, F., 1977: Variable fine mesh in spectral global model. Beitr. Phys. Atmos., **50**, 211-217.

Sharma, O. P., H. Upadhyaya, Th. Braine-Bonnaire and R. Sadourny, 1977: Experiments on regional forecasting using a stretched coordinate general circulation model. Short- and Medium- Range Numerical Weather Prediction: Collection of Papers Presented at the WMO/IUGG NWP Symposium, Tokyo, 4-8 August 1986, Special Volume of J. Meteor. Soc. Japan, Ed. T. Matsuno, 263-271.

Sharman, R. D., T. L. Keller and M. G. Wurtele, 1988: Incompressible and anelastic flow simulations on numerically generated grids. Mon. Wea. Rev., **116**, 1124-1136.

Simmons, A. J., and D. M. Burridge, 1981: An energy and angular-momentum conserving vertical finite-difference scheme and hybrid vertical coordinates. Mon. Wea. Rev., 109, 758-766.

Simmons, A. J., and R. Strüfing, 1981: An energy and angular-momentum conserving finite-difference scheme, hybrid coordinates and medium-range weather prediction. Tech. Rep. No. 28, ECMWF, Shinfield Park, Reading, U.K.

Skamarock, W. C., 1989: Truncation error estimates for refinement criteria in nested and adaptive models. Mon. Wea. Rev., **117**, 872-886.

Skamarock, W. C., and J. B. Klemp, 1989: Adaptive models for 2-D and 3-D nonhydrostatic atmospheric flow. Preprints, Sixth Int. Conf. on Num. Methods in Laminar and Turbulent Flow, Suansea, Wales, U.K.

Skamarock, W., J. Oliger and R. L. Street, 1989: Adaptive grid refinement for numerical weather prediction. J. Comput. Phys., **80**, 27-60.

Smolarkiewicz, P. K., 1983: A simple positive definite advection scheme with small implicit diffusion. Mon. Wea. Rev., **111**, 479-486.

Smolarkiewicz, P. K., 1984: A fully multidimensional positive definite advection transport algorithm with small implicit diffusion. J. Comput. Phys., **54**, 325-362.

Staniforth, A., and H. Mitchell, 1978: A variable resolution finite element technique for regional forecasting with the primitive equations. Mon. Wea. Rev., **106**, 439-447.

Takacs, L. L., 1988: Effects of using a posteriori methods for the conservation of integral invariants. Mon. Wea. Rev., **116**, 525-545.

Takacs, L. L., and R. C. Balgovind, 1983: High-latitude filtering in global grid-point models. Mon. Wea. Rev., **111**, 2005-2015.

Tuccillo, J. J., 1988: Parameterization of physical processes in NMC's Nested Grid Model. Preprints, Eighth Conf. Numerical Weather Prediction, Baltimore, Amer. Meteor. Soc., 238-243. [Boston, MA 02108.]

Van Leer, B., 1977: Towards the ultimate conservative difference scheme. V. A new approach to numerical convection. J. Comput. Phys., **23**, 276-299.

Van Leer, B., 1979: Towards the ultimate conservative difference scheme. IV. A second-order sequel to Godunov's method. J. Comput. Phys., **32**, 101-136.

Williamson, D. L., 1979: Difference approximations for fluid on a sphere. Numerical Methods used in Atmospheric Models. GARP Publ. Ser., No. 17, Vol. II, WMO, Geneva, 51-120. [Pub. WMO/ICSU, Case Postale No. 2300, CH-1211 Geneva 20, Switzerland.]

Williamson, D. L., and P. J. Rasch, 1988: Shape preserving interpolators for semi-Lagrangian transport. Techniques for Horizontal Discretization in Numerical Weather Prediction Models. Workshop 1987, ECMWF, Shinfield Park, Reading, U.K., 117-141.

Williamson, D. L., and P. J. Rasch, 1989: Two-dimensional semi-Lagrangian transport with shape-preserving interpolation. Mon. Wea. Rev., **117**, 102-129.

WMO/ICSU, 1979: Numerical Methods used in Atmospheric Models. GARP Publ. Ser., No. 17, Vol. II, WMO, Geneva, 500 pp. [Pub. WMO/ICSU, Case Postale No. 2300, CH-1211 Geneva 20, Switzerland.]

Winninghoff, F. J., 1968: On the adjustment toward a geostrophic balance in a simple primitive equation model with application to the problems of initialization and objective analysis. Ph. D. Thesis, Dept. Meteor. Univ. California, Los Angeles, CA 90024.

Zalesak, S. T. 1979: Fully multidimensional flux-corrected transport for fluids. J. Comput. Phys., **31**, 335-362.